TECHNISCHE UNIVERSITÄT MÜNCHEN

Lehrstuhl für Grünlandlehre

Kinetic Characterisation of Respiratory Carbon Pools in a Grassland Ecosystem

Ulrike Gamnitzer

Vollständiger Abdruck der von der Fakultät Wissenschaftszentrum Weihenstephan für Ernährung, Landnutzung und Umwelt der Technischen Universität München zur Erlangung des akademischen Grades eines

Doktors der Naturwissenschaften

genehmigten Dissertation.

Vorsitzender:		Univ.-Prof. Dr. E. Grill
Prüfer der Dissertation:	1.	Univ.-Prof. Dr. J. Schnyder
	2.	Univ.-Prof. Dr. R. Matyssek
	3.	Assoc. Prof. D.R. Bowling, Ph.D., University of Utah, Salt Lake City/USA (schriftliche Beurteilung)

Die Dissertation wurde am 22.12.2009 bei der Technischen Universität München eingereicht und durch die Fakultät Wissenschaftszentrum Weihenstephan für Ernährung, Landnutzung und Umwelt am 24.02.2010 angenommen.

Summary

Aims. The subject of the present study was the kinetic characterisation of the respiratory substrate supply in a grassland ecosystem. For this purpose, a methodology was developed for generation and analysis of tracer kinetics in ecosystem respiration in the field. Specifically, the relative contributions and the turnover of the main carbon sources were studied. Discrepancies between belowground respiratory CO_2 production and soil CO_2 efflux were of particular interest, as they are relevant for the measurement accuracy.

Material & Methods. The apparatus for continuous labelling at ambient CO_2 concentration included four open-top chambers, flushed with a mix of CO_2-free air and ^{13}C-depleted CO_2, a CO_2 analyser and an online isotope-ratio mass spectrometer. Nighttime measurements of the tracer content in ecosystem respiration were accomplished with the chambers operated in both open (steady-state flow-through) and closed (non-steady-state CO_2 accumulation) mode. Mechanisms underlying discrepancies between the two chamber modes were investigated with a soil CO_2 transport model, which accounted for diffusion of $^{12}CO_2$ and $^{13}CO_2$ in the soil, dissolution of CO_2 in soil water and mass displacement of soil air. From the observed tracer time course in ecosystem respiration, the kinetic characteristics of substrate pools were determined with compartmental analysis.

Results & Discussion. In the open-top chambers, the isotopic composition of CO_2 was stable ($\delta^{13}C = -46.9 \pm 0.4‰$) during photosynthetic tracer uptake, and CO_2 concentration and climatic conditions represented natural conditions. The accuracy of the open-mode respiration measurements was supported by an independent, laboratory-based reference system. Compared to that, closed-mode measurements suggested a ∼1.5-fold tracer content in ecosystem respiration. 82% of this bias were explained by changed CO_2 composition in the closed chamber headspace, dissolution of labelling CO_2 in soil water and displacement of soil air. This indicated that penetration of tracer into soil pores during tracer application and release into chamber air during the subsequent closed-mode measurement significantly biased the observations. The 'true' (open-mode derived) tracer kinetics fitted a two-source model: 48% of the observed ecosystem respiration were supplied by a rapidly labelled source with a mean residence time of C of 3.7 d. This source was closely connected with autotrophic respiration. The other source contributed 52% of respiration and released no tracer during 14 days of labelling. It was associated with heterotrophic

decomposition of structural plant biomass.

Conclusions. The kinetic characteristics of autotrophic respiration observed in the field are consistent with current understanding of plant and stand-scale respiration gained in controlled environment experiments. This suggests, that the methodology established in the present work is a valuable tool to study ecosystem functioning.

Zusammenfassung

Zielsetzung. Die vorliegende Arbeit befasst sich mit der kinetischen Charakterisierung der respiratorischen Substratversorgung in einem Graslandökosystem. Es wurde eine Methodik zur Erzeugung und Analyse von Markierungskinetiken in Ökosystemrespiration im Feld entwickelt. Insbesondere wurden die relativen Beiträge und der Turnover der Hauptquellen des Kohlenstoffs untersucht. Dabei waren Unterschiede zwischen unterirdischer, respiratorischer CO_2-Produktion und dem Fluss von CO_2 aus dem Boden von speziellem Interesse, da diese für die Exaktheit von Messungen entscheidend sind.

Material & Methoden. Die Apparatur für kontinuierliche Markierung bei natürlicher CO_2-Konzentration bestand aus vier „Open-Top"-Kammern, die mit einer Mischung aus CO_2-freier Luft und CO_2 gespült wurden, einem CO_2-Analysator und einem Online-Isotopenverhältnis-Massenspektrometer. Nächtliche Messungen des Markierungsgehalts in der Ökosystemrespiration wurden mit den Kammern durchgeführt, wobei diese sowohl im offenen (steady-state Durchfluss) als auch im geschlossenen (non-steady-state CO_2-Akkumulation) Modus betrieben wurden. Die Mechanismen hinter Unterschieden zwischen den beiden Kammermodi wurden mit einem Boden-CO_2-Transportmodell untersucht, welches die Diffusion von $^{12}CO_2$ und $^{13}CO_2$ im Boden, die Lösung von CO_2 im Bodenwasser und die Verschiebung von Bodenluftmassen berücksichtigte. Aus der beobachteten Markierungszeitreihe der Ökosystemrespiration wurden die kinetischen Eigenschaften der Substratpools mit kompartimenteller Analyse bestimmt.

Ergebnisse & Diskussion. In den Open-Top-Kammern war die isotopische Zusammensetzung des CO_2 ($\delta^{13}C = -46.9 \pm 0.4‰$) während der photosynthetischen Traceraufnahme stabil, und die CO_2-Konzentration und die klimatischen Bedingungen entsprachen natürlichen Bedingungen. Die Exaktheit der Respirationsmessungen im offenen Kammermodus wurde durch ein unabhängiges, laborbasiertes Referenzsystem belegt. Im Vergleich dazu zeigten die Messungen im geschlossenen Kammermodus den ∼1.5-fachen Markierungsgehalt. 82% dieses systematischen Fehlers konnten durch Änderungen in der CO_2-Zusammensetzung der Luft in der geschlossenen Kammer, die Lösung von Markierungs-CO_2 im Bodenwasser und die Verschiebung von Bodenluftmassen erklärt werden. Dies deutete darauf hin, dass die Markierung, die während ihrer Applikation in die Bodenporen eindrang und während der nachfolgenden Messung wieder freigesetzt wurde, die

Messung im geschlossenen Modus signifikant beeinflusste. Die „wahre“ Markierungskinetik (bestimmt im offenen Kammermodus) entsprach einem Zwei-Pool-Modell: 48% der gemessenen Ökosystemrespiration stammten aus einer rasch markierten Quelle mit einer mittleren Verweildauer für Kohlenstoff von 3.7 d. Diese Quelle war eng mit autotropher Respiration verbunden. Die andere Quelle trug 52% zur Respiration bei und setzte während der zweiwöchigen Markierungsdauer keinen Tracer frei. Sie war mit heterotropher Zersetzung von struktureller Pflanzenbiomasse verknüpft.

Schlussfolgerungen. Die im Feld beobachteten kinetischen Eigenschaften der autotrophen Respiration stehen im Einklang mit dem gegenwärtigen Verständnis von Pflanzen- und Bestandesrespiration, das in Experimenten unter kontrollierten Bedingungen gewonnen wurde. Dies deutet darauf hin, dass die Methodik, die in der vorliegenden Arbeit eingeführt wurde, ein nützliches Werkzeug zur Untersuchung der Funktionsweise von Ökosystemen ist.

Contents

List of Figures

List of Tables

1 General introduction

The present work deals with the kinetic characterisation of respiratory carbon (C) pools in a temperate grassland ecosystem. Respiration is indispensable to the life of most organisms (because it makes energy available to sustain an organism's vital functions), and requires C in form of organic compounds. These organic compounds were previously synthesised from photosynthetically fixed C. Under consumption of oxygen (O_2) and gain of energy in form of adenosine triphosphate (ATP), they are transformed into carbon dioxide (CO_2), which is released back to the atmosphere. In an ecosystem, the ways C can take between its photosynthetic fixation and respiratory release are manifold and differ in the time lag between fixation and release, the residence time. For example, recently assimilated C can be utilised in plant respiration, resulting in a short residence time (hours to days). C built into structural plant biomass can remain in the ecosystem for months to centuries before the organic matter is decomposed by heterotrophs. Hence, the residence time of C is determined by its allocation within the plant-soil continuum and by the kinetics of the associated C pools. Investigation of the residence time can reveal information on mechanisms behind ecosystem C cycling and ecosystem functioning.

Grassland ecosystems play an important role in the global C cycle, as their soil and vegetation contains about one third of the total C stored in terrestrial ecosystems (White *et al.*, 2000). Grasslands cover approx. 40% of the world's land area (excluding Antarctica and Greenland) — much more than other agroecosystems or forests (White *et al.*, 2000). However, C allocation may differ between plant functional groups and biomes. Thus understanding C cycling in grasslands contributes to the understanding of global C cycling.

Methodological aspects of characterising ecosystem C turnover

A useful experimental technique to study the fate of C on its way through an ecosystem is to label the photosynthetic flux and thus the incorporated C. When this labelled

C is allocated to a pool supplying respiration, it will occur in respired CO_2 and can be detected there. The time course of tracer in respired CO_2 (the tracer kinetics) carries information about the kinetic characteristics of the involved pools. Changing the isotopic composition of assimilated C is well suited for labelling, because it does not disturb the metabolic pathways within the ecosystem. An isotopic tracer widely used in ecological research is ^{13}C (Griffiths, 1991; Dawson *et al.*, 2002), the only stable C isotope besides the most abundant ^{12}C. With continuous-flow isotope-ratio mass spectrometers, a convenient measurement technique is available for observing the tracer, even online in the field (Schnyder *et al.*, 2004). Continuous application of the tracer causes all involved substrate pools to change their tracer content (therefore also termed 'dynamic labelling' (Ratcliffe & Shachar-Hill, 2006)) until finally a new isotopic equilibrium is reached ('steady-state labelling' (Geiger, 1980)). This enables detection of sources with different turnover rates (de Visser *et al.*, 1997; Thornton *et al.*, 2004) compared to pulse labelling, where rapidly turned over pools receive more tracer than slower ones (Geiger, 1980; Meharg, 1994). Furthermore, near-natural abundance $^{13}CO_2/^{12}CO_2$ is well suited for continuous labelling, while pulse labelling studies usually require highly ^{13}C-enriched tracer due to dilution of the tracer signal on its way through the ecosystem.

Continuous labelling at ambient CO_2 concentration in the field can be achieved by enclosing the ecosystem in an open chamber which is flushed with air containing the tracer. The tracer can be obtained by mixing CO_2-free air with CO_2 of the desired isotopic composition (Deléens *et al.*, 1983), which was proved successfully in laboratory labelling studies (Schnyder, 1992; Schnyder *et al.*, 2003). Precise labelling requires exposure of the ecosystem to constant and homogeneous atmospheric CO_2 concentration and isotopic composition during the whole period of tracer uptake. Thus, the inevitable feedback of the enclosed ecosystem on chamber headspace CO_2 due to assimilation, respiration and associated isotopic discrimination (Farquhar & Lloyd, 1993) needs to be minimised. Furthermore, climatic conditions such as temperature, humidity and light inside the chamber should represent natural conditions.

Observing the tracer kinetics in nighttime ecosystem respiration requires non-destructive, precise and accurate measurement of the isotopic composition of respired CO_2. Among chamber techniques applied in the field to determine the isotopic composition of soil and ecosystem respired CO_2, open (steady-state flow-through; classification according to Livingston & Hutchinson, 1995) chambers (e.g. Subke *et al.*, 2009) are the most convenient. They are operated in the same way as during daytime tracer application and thus ensure

minimal disturbance. Closed (non-steady-state non-flow-through) chambers (Søe *et al.*, 2004; Ohlsson *et al.*, 2005) in combination with Keeling plots (Keeling, 1958) are the least complex system to be considered. Closed chambers at steady-state (Mora & Raich, 2007) are inappropriate for the present study: achievement of steady-state most likely takes several days (Kayler *et al.*, 2008), which impedes the observation of tracer kinetics in the first few days following the onset of labelling. However, suitability in terms of accuracy needs to be verified, because chamber measurements are potentially biased by pressure differences between chamber headspace and surrounding air (Fang & Moncrieff, 1998; Lund *et al.*, 1999), ambient air incursion into the chamber headspace (Baldocchi *et al.*, 1989) and disturbance of the soil CO_2 gradient beneath the chamber (Ohlsson *et al.*, 2005; Nickerson & Risk, 2009c). Subke *et al.* (2009) recently reported non-biological tracer return from the soil pore spaces in a pulse-chase experiment, where the tracer was highly enriched in ^{13}C. To what extent this can confound tracer observations in a continuously labelled environment, where the tracer shows near-natural abundance $^{13}CO_2/^{12}CO_2$ ratio, has not yet been investigated.

Substrate supply to ecosystem respiration

C pools supplying respiration have been studied on different scales under controlled conditions, particularly in leaves (Nogués *et al.*, 2004), root and shoot (Lehmeier *et al.*, 2008), whole plants (Ryle *et al.*, 1976; Lehmeier *et al.*, 2010) and mesocosms (Schnyder *et al.*, 2003). However, complementary investigations in the field are inevitable to verify the mechanisms, which were detected in artificial environments, in natural conditions and permit extrapolation to the ecosystem level. Previous field studies surveyed C cycling mainly at elevated CO_2 concentration by using free air carbon-dioxide enrichment (FACE) technology, e.g. respiratory substrate supply to belowground respiration in forest (Pregitzer *et al.*, 2006; Taneva *et al.*, 2006), grassland (Torn *et al.*, 2003) and cropland ecosystems (Søe *et al.*, 2004). At ambient CO_2 concentration, pulse-chase tracer techniques were applied to investigate the residence time of C in forests (Carbone *et al.*, 2007; Högberg *et al.*, 2008) and grasslands (Ostle *et al.*, 2000; Johnson *et al.*, 2002; Carbone & Trumbore, 2007; Bahn *et al.*, 2009; Subke *et al.*, 2009). Continuous labelling facilitates the assessment of substrate pools with different turnover times and hence is expected to further increase our understanding of substrate supply to ecosystem respiration. However, it has not yet been applied at ambient CO_2 concentration in the field. This is partly due to a lack of

a suitable methodology. The present study aims to close this gap by introducing a new labelling technology for field use.

Studies of *Lolium perenne* under controlled conditions revealed mean residence times of C in the respiratory substrate supply system between 3.6 and 9.2 d for individual plants (Lehmeier *et al.*, 2008, 2010) and on the stand-scale (Schnyder *et al.*, 2003). Furthermore, Thornton *et al.* (2004) determined that half of exudate C from the same species was turned over within 4.5 d. The estimate of 4.8–8.2 d for the mean age of C respired by a California mountain grassland ecosystem, derived from pulse labelling, (Carbone & Trumbore, 2007) is consistent with these findings. Hence, a 2 weeks period of continuous labelling should allow (1) separation of the two major substrate pools supplying ecosystem respiration in a grassland — namely recently assimilated C from plant and rhizosphere respiration, and 'old' C from litter decomposition — and (2) assessment of the turnover of the former.

Overview and aims

All field measurements reported in the present study were carried out in a temperate humid grassland ecosystem. The study site was located at Grünschwaige Grassland Research Station, on a permanent pasture. The vegetation was dominated by the C3 grasses *Lolium perenne* and *Poa pratensis*.

First of all, this study aimed to provide a $^{13}CO_2/^{12}CO_2$ tracer technique for continuous labelling at ambient CO_2 concentration and online measurements of ecosystem CO_2 fluxes in the field. A novel open-top chamber system was established to allow for constant and homogeneous tracer application at near-ambient climatic conditions. The open-chamber system — operated at steady-state — was tested upon its suitability to accurately measure the tracer content in nighttime ecosystem respiration. The time course of tracer was analysed during two weeks of continuous labelling. This observed tracer kinetics was interpreted with a simple compartmental model, with particular respect to partitioning of ecosystem respiration and the residence time of assimilated C in the system (Chapter 2).

Secondly, non-steady-states of the soil CO_2 pool were explored. This is of particular interest, because approaches aiming to measure the isotopic signal of belowground respiration commonly access CO_2 emerging from the soil surface, after it has passed through the soil pores. A quantitative analysis was performed to clarify the mechanisms behind this process by using a soil CO_2 transport model. This accounted for diffusion of $^{12}CO_2$ and

$^{13}CO_2$, dissolution of CO_2 in soil water and mass flow of soil air. Implications of these mechanisms for commonly applied isotopic approaches were considered (Chapter 3).

Finally, advantages, limitations and potential applications of the new tracer technique are discussed, with particular respect to the investigation of seasonal and interannual variations in C cycling (Chapter 4).

2 Observing ^{13}C labelling kinetics in CO_2 respired by a temperate grassland ecosystem*

Summary

The kinetic characteristics of the main sources of ecosystem respiration are quite unknown, partly due to methodological constraints. We present a new open-top chamber (OTC) apparatus for continuous $^{13}C/^{12}C$ labelling and measurement of ecosystem CO_2 fluxes, and report the tracer kinetics of nighttime respiration of a temperate grassland.

The apparatus includes four dynamic flow-through OTCs, a unit mixing CO_2-free air with ^{13}C-depleted CO_2, and a CO_2 analyser and an online isotope ratio mass spectrometer.

The concentration ($367 \pm 6.5\,\mu mol\,mol^{-1}$) and carbon isotopic composition, $\delta^{13}C$, ($-46.9 \pm 0.4‰$) of CO_2 in the OTCs was stable during photosynthesis due to high air throughflux and minimal incursion through the buffered vent. Soil CO_2 efflux was not affected by pressure effects during respiration measurements. The labelling kinetics of respiratory CO_2 measured in the field agreed with that of excised soil+vegetation blocks measured in a laboratory-based system. The kinetics fitted a two-source system ($r^2 = 0.97$), with a rapidly labelled source ($T_{1/2} = 2.6\,d$) supplying 48% of respiration, and the other source (52%) releasing no tracer during 14 days of labelling.

Of the two sources supplying ecosystem respiration, one was closely connected with current photosynthesis (≈ autotrophic respiration) and the other was provided by decomposition of structural plant biomass (≈ heterotrophic respiration).

* Gamnitzer U, Schäufele R, Schnyder H (2009) *New Phytologist* **184:** 376–386

Introduction

This work is concerned with the kinetics of substrate supply to ecosystem respiration in a temperate grassland system. In grasslands, as in other ecosystems, most of the carbon (C) fixed in photosynthesis is eventually returned to the atmosphere by way of autotrophic or heterotrophic respiration. However, there is an enormous variation in the time lag between C fixation and release. For example, if current photosynthate is used in root respiration, then the residence time of C in the system is short (hours to days); but if C is incorporated in structural compounds then the residence time is long (months to centuries) (Högberg & Read, 2006). So, the residence time of C in the biosphere is a function of allocation. Knowledge of (respiratory substrate) C allocation and associated pool kinetics is important for understanding C cycling and ecosystem C storage (Trumbore, 2006).

Manipulation and monitoring of the isotopic composition of assimilated C is a way to trace C on its way through an ecosystem with no (or minimal) disturbance of photosynthesis, allocation and respiration. Turnover of respiratory C pools has mainly been studied in controlled environments at different levels of biological integration: leaves (Nogués *et al.*, 2004), root and shoot (Lehmeier *et al.*, 2008), whole plants (Ryle *et al.*, 1976), and mesocosms (Schnyder *et al.*, 2003). However, field labelling studies are essential to allow mechanisms detected in artificial environments to be assessed in natural conditions and at the ecosystem level. Field studies have investigated the residence time of C or respiratory labelling kinetics (the time course of tracer in respired CO_2) with pulse-chase tracer techniques in forest (Carbone *et al.*, 2007; Högberg *et al.*, 2008) and grassland ecosystems (Ostle *et al.*, 2000; Johnson *et al.*, 2002; Carbone & Trumbore, 2007; Bahn *et al.*, 2009). Pulse labelling causes strong labelling of rapidly turned over pools, but weak labelling of slowly turned over pools (Geiger, 1980; Meharg, 1994), impeding the assessment of the slow pools' contribution to respiration. Continuous labelling (also termed 'dynamic labelling' (Ratcliffe & Shachar-Hill, 2006), or — more classically — 'steady-state labelling' (Geiger, 1980) in plant biology literature) avoids this complication: the amount of tracer in respired CO_2 increases until — eventually — all substrate pools of respiration have reached isotopic equilibrium. The kinetics of this increase reflects the functional properties of the pool system supplying respiration (number and arrangement of pools, and the size, turnover rate and contribution of individual pools to the total respiratory flux), which can be uncovered by compartmental analysis (Atkins, 1969; Jacquez, 1996).

To our knowledge, no technique for continuous labelling at ambient CO_2 in the field has yet been described. For this plants must be exposed to an atmosphere with a C isotopic composition of CO_2 that is different from natural conditions but constant and homogeneous during daylight hours. For labelling at ambient CO_2, manipulation of the isotopic composition can be achieved by enclosing the ecosystem in an open chamber (more exactly termed steady-state flow-through system, see Livingston & Hutchinson, 1995), flushed with air containing CO_2 of the desired C isotopic composition. The technique should ensure that the concentration and isotopic composition of CO_2 in the chamber headspace is not significantly altered by photosynthesis and respiration and associated isotopic discrimination. Ideally, climatic conditions inside the chamber should not differ from the natural conditions.

The most obvious method for non-destructive, in situ detection of tracer in respired CO_2* is the analysis of gas exchange in an open chamber system, in combination with online C isotope analysis. In such a system, dark respiration rate is quantified as the difference between chamber inlet and outlet CO_2 fluxes. Analogously, the isotopic composition of respired CO_2 is assessed from isotopic mass balance of inlet and outlet CO_2 fluxes. Such measurements are susceptible to artefacts such as ambient air incursions and pressure effects. To minimise incursion, Baldocchi *et al.* (1989) recommended decreasing the size of the chamber opening below the length scale of turbulence elements and increasing the velocity of air exiting through the top (v_{exit}) to oppose the entraining ambient air. However, increasing v_{exit} can cause pressure effects which reduce soil CO_2 efflux considerably: overpressure of less than 1 Pa can suppress soil CO_2 efflux by more than 50% (Fang & Moncrieff, 1998; Lund *et al.*, 1999; see also Kanemasu *et al.*, 1974). Thus, chamber design and operating conditions must minimise the conflict between air incursion and pressure artefacts.

In this paper we present a new system, based on open-top chambers (OTC), for the continuous application of a $^{13}CO_2/^{12}CO_2$ tracer on grassland ecosystems and the quasi-continuous online-measurement of the tracer in ecosystem respiration in the field. To assess its performance, we investigated (1) the constancy and homogeneity of the concentration and isotopic composition of CO_2 inside the chambers, (2) effects of chamber design and operating conditions on air incursion and on the accuracy of measurement of

* Here a conceptual distinction between belowground respiratory CO_2 production and soil CO_2 efflux is not made, as they are considered to be equal. For a detailled discussion of the difference see Chapter 3 for further discussion.

respiratory CO_2, including pressure effects, and (3) environmental conditions inside the OTCs. Then, (4) we measured the tracer kinetics of respiration in a temperate grassland ecosystem during a 16 days-long labelling interval and (5) compared these field respiration measurements with laboratory-based (reference) measurements of excised soil+vegetation blocks. Finally, (6) we analyse and interpret the tracer kinetics with a simple compartmental model.

Materials and Methods

Open-top chamber system for labelling and respiration measurement

The chamber system, schematically shown in Fig. 2.1, consisted of three main parts: (1) four OTCs, (2) a unit supplying air of desired CO_2 concentration and isotopic composition, and (3) the gas exchange measurement unit, including sample selection, infrared gas analyser for CO_2 and water vapour concentration analysis, and a continuous-flow isotope-ratio mass spectrometer for analysis of $^{13}CO_2$.

The chambers consisted of clear acrylic glass (Plexiglas XT 20070, 4 mm thick, Röhm Degussa, Darmstadt, Germany; for transparency to photosynthetic active radiation see 'Characterisation of chamber properties'). The chamber body had cylindrical shape, based on an octagon of 100 cm diameter, resulting in a chamber base area, A_{chamber}, of 0.83 m^2. Chamber body height was 80 cm, and the volume 660 l. A removable horizontal plate with a hole in the middle was placed on top of the cylindrical body. In addition, a removable open frustrum with 30° angle was placed on the cylinder. In the final configuration the diameter of the opening in both top parts could be adjusted between 6.5 and 32 cm, corresponding to 0.4–10% of the chamber base area.

To separate the enclosed part of the ecosystem from the surrounding environment, the chamber was placed on a 15 cm high stainless steal collar, which was forced about 12 cm into the soil. A water-filled channel on top of the collar provided sealing between the collar and the chamber body. Some of the chamber tests were performed with the chamber bottom sealed with a plastic or stainless steal plate to exclude soil and vegetation signals.

To supply the chambers with air of desired CO_2 concentration and isotopic composition, the principle introduced by Deléens *et al.* (1983) was followed: CO_2-free dry air was generated at a rate of about 3200 standard liter per minute (SLPM) using a screw compressor

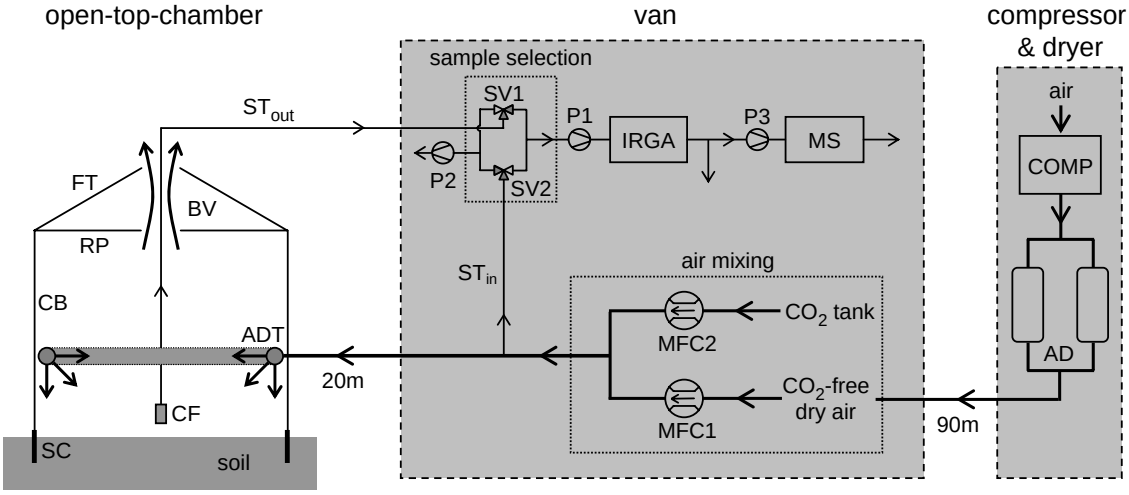

Figure 2.1: Schematic diagram of the chamber system consisting of open-top chamber (CB, chamber body; RP, removable plate; FT, frustrum top; BV, buffer volume; SC, soil collar), air supply unit (COMP, screw compressor; AD, adsorption dryer; MFC1, mass flow controller for air flow; MFC2, mass flow controller for CO_2 flow; ADT, air distribution tube) and gas exchange observation unit (ST_{in}/ST_{out}, sampling tubes for chamber inlet/outlet; CF, coarse filter; SV1 and SV2, 3 way solenoid valves for sample selection; P1, sample pump; P2, bypass pump; IRGA, infrared gas analyser; P3, mass spectrometer sample air pump; MS, gas chromatographic column and isotope ratio mass spectrometer). Thick lines indicate flow to/through the chamber, thin lines indicate sample air flow. For clarity only one (out of four) open-top chamber with its air mixing system and sample selection valves is shown. All chambers had their own gas mixing unit, and gas supply and sampling air lines.

(A50-H8, Babatz, Bad Wimpfen, Germany) which fed an adsorption dryer (KEN 3100, Zander, Essen, Germany). The CO_2-free dry air was conveyed to a mixing unit, housed 90 m away in an air-conditioned van, via a polyethylene (PE) tube which was burried in the soil at 70 cm depth. Each chamber was equipped with a separate mixing unit, consisting of one mass flow controller (Bronkhorst Hi Tec, Ruurlo, The Netherlands; 0–1000 SLPM), which controlled the flow of CO_2-free air, and another mass flow controller (Millipore, Billerica, MA, USA; 0–1 SLPM), which controlled the amount of CO_2 added to the air stream from a high pressure cylinder. Maximum air flow per chamber was 800 SLPM when all four chambers were operated. The chambers were connected with their mixing units via flexible tubes (PVC fabric tube, length ≤ 20 m, inner diameter 32 mm). Air distribution in the OTC was achieved with a circular tube (circle diameter 93 cm, tube inner diameter 32 mm) mounted at about 30 cm height inside the chamber. The tube contained 46 holes (8 mm diameter) which directed the air downwards, inwards and diagonally downward-inwards. To avoid excessive warming of the air inside the OTCs due to the greenhouse

effect, the air supplied to the OTCs was cooled by burrying the tube upstream of the mixing unit in the soil, expanding the air from 0.7 MPa to ambient air pressure in the mixing unit, and thermally isolating the downstream air supply tubes. Transpiration by the canopy and evaporation by the soil inside the OTC contributed further cooling.

For analysis of CO_2 the chamber inlet was sampled with a teflon (polytetrafluoroethylene, PTFE) tube which diverged from the chambers air supply immediately after the mixing unit. Outlet air was sampled inside the chamber using a PTFE tube which was equipped with a coarse filter. Each chamber was equipped with its own sampling tubes. The sample tubes of the chamber inlets and outlets were connected to a system of three-way solenoid valves which allowed selection of one (out of a total of eight; two per chamber) sample tube for analysis, while the other tubes were flushed. This enabled rapid sequential analysis of all eight sample lines with one set of analysers. Sample air from the selected line was drawn with a membrane pump at approx. 1.6 SLPM and passed on to an infrared gas analyser (IRGA, LI 7000, LiCor, Lincoln, Nebraska, USA) and continuous-flow isotope-ratio mass spectrometer (Delta Plus Advantage, Thermo Electron, Bremen, Germany) interfaced with a gas chromatic column (Gasbench II, Thermo Electron, Bremen, Germany) (Schnyder *et al.*, 2004). Carbon isotopic compositions are presented as $\delta^{13}C = R_{sample}/R_{standard} - 1$, where R_{sample} and $R_{standard}$ are the $^{13}C/^{12}C$ ratios in the sample and in the international VPDB standard. All mass spectrometric measurements were corrected for linearity effects (i.e. dependence of the raw ^{13}C value on the actual CO_2 concentration) according to measurements of a laboratory standard CO_2, mixed in CO_2-free air at different concentrations. The sample selection unit and the measurement instrumentation were placed in a temperature-controlled van.

Each chamber was equipped with a set of sensors for environmental conditions, including air temperature/relative humidity (1400 104, LiCor), soil temperature (1400 103, LiCor) and photosynthetic photon flux density PPFD (LI 190SZ quantum sensor interfaced with photomultiplier MV 100, LiCor). Each air temperature/relative humidity sensor was mounted in a double-walled, ventilated housing. The sensors agreed within 0.2 °C (SD) air temperature and 0.5% (SD) relative humidity when exposed to the same environment. PPFD sensors were installed horizontally and agreed within 11 µmol m^{-2} s^{-1} (SD).

For central control of the system and data acquisition, the flow controllers, the environmental conditions sensors, the sample selection valves and the IRGA were connected to a PC via Field Point communication modules (National Instruments, Austin, TX, USA).

Setting of flow rates and automated sample selection as well as data logging for the selected sample line on a 1-s basis were performed with custom-built software (Walz, Effeltrich, Germany). As the mass spectrometer was equipped with a separate PC, synchronisation of mass spectrometer sampling intervals with sample selection times was carried out by means of a trigger.

All measurements were carried out in a temperate humid grassland at Grünschwaige Grassland Research Station (Schnyder *et al.*, 2006). The chamber system was placed in the middle of paddock number 8. An eddy-covariance system was located near the van and logged 3D wind speed (CSAT 3, Campbell Scientific, Logan, Utah, USA) and CO_2 concentration (LI 7500, LiCor) at 1.5 m height (H. Schnyder, unpublished data).

Characterisation of chamber properties

Mixing of chamber air. To quantify the distribution of incoming air within the chamber, an empty OTC (opening size 0.4% of chamber base area) with impermeable base was flushed with CO_2-free dry air at 100 SLPM (which was close to the lower limit of adjustable air flows). Then, CO_2 concentration in the incoming air was suddenly increased to 1000 µmol mol^{-1} and, after nearly reaching this value in the chamber air, suddenly decreased back to 0 µmol mol^{-1}. The change of CO_2 concentration following the concentration switches was tracked at twelve positions distributed horizontally and vertically over the chamber cross section (see Fig. 2.2) for 25–30 min. This was done by installing the chamber outlet sampling tube and taking IRGA readings, consecutively at each of the positions.

Ambient air incursion. An empty OTC with impermable base was also used to quantify the amount of ambient air blown into the chamber through the open top. For this, the chamber was continuously flushed with CO_2-free dry air, and CO_2 concentration inside (25 cm sampling height) and outside the chamber was monitored. The ratio of ambient air to total air inside the chamber ($air_{amb}/air_{chamber}$) was given by the ratio of CO_2 concentration inside the chamber to CO_2 concentration in ambient air.

Pressure effects on soil CO_2 efflux. The disturbance of soil CO_2 efflux by chamber pressure effects was investigated with a OTC placed on a grassland ecosystem section from which the above ground biomass had been completely removed. All observations

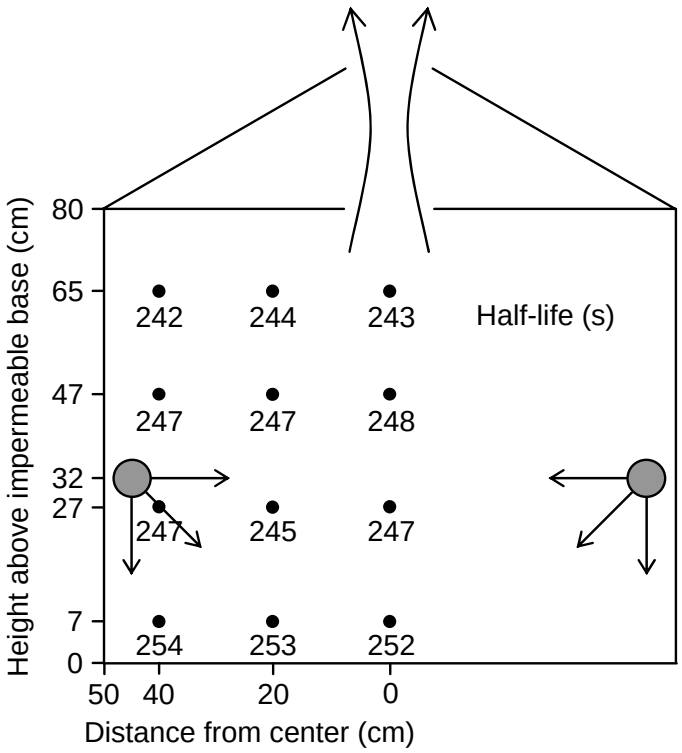

Figure 2.2: Half-lives of CO_2 concentration changes in chamber air, following abrupt changes in CO_2 concentration of the incoming air. Black dots indicate the observation positions in the chamber cross section; arrows indicate the air flow.

were completed within 6 h after shoot removal. The chamber, set up with different top opening sizes, was flushed with air at different flow rates, providing a range of chamber exit velocities, v_{exit}. Soil CO_2 efflux rate was calculated from the CO_2 concentration difference between chamber inlet and outlet, and the rate of air flow through the OTC, according to Eqn. 2.1. Simultaneously with CO_2 efflux rate, the pressure difference between inside and outside of the OTC, $p_{\text{diff}} = p_{\text{inside}} - p_{\text{outside}}$, was monitored by connecting the sample port of a differential pressure sensor (LP 8000, Druck Limited, Leicester, UK) with the chamber inside via a tube, while the sensor's reference port was exposed to ambient air.

Light transmission. Light transmission of the OTC was quantified with PPFD sensors mounted on eight different places spread over the chamber cross section at plant canopy height and a reference sensor mounted outside the chamber. Light attenuation by the OTC occured due to reflection by the chamber wall material and due to partial shading caused by installations like air supply and sampling tubes. Mean light transmission of the chamber system was 82% in sunny conditions.

Protocol of labelling experiment

In May 2007 a 16 days-long labelling experiment was performed on a part of the pasture that had recovered from grazing for about two weeks. For site conditions see Schnyder *et al.* (2006). 5–10 d before the start of labelling, soil collars were installed at ten selected sites. The vegetation at all sites was dominated by *Lolium perenne* L., *Poa pratensis* L., *Trifolium repens* L. and *Taraxacum officinale* L. and had a mean canopy height of 6–7 cm. Tracer was applied during daytime hours and ecosystem respiration was measured online in the field during nighttime hours. First respiration measurements were made in the night before the start of the labelling experiment, to obtain the isotopic signature of respiration from the non-labelled ecosystem. Measurements were continued every night for the entire duration of labelling. Sites were labelled individually for periods of 1, 2, 4, 8 or 16 days, with two replications each. All labelling was performed within a 16 days period, using four OTCs. Two OTCs served to label two sites for the entire 16 days-long period, and the other two OTCs rotated between sites for the shorter labelling durations. This sampling scheme was chosen to allow for the direct comparison of (non-destructice) in-situ and reference measurements (which required the sampling of the labelled vegetation, see 'Reference measurements' below).

Daytime labelling. Labelling started in the early morning by placing an OTC (opening size 1% of chamber base area) on a soil collar. For the desired number of labelling days, the chamber was flushed from 5:30 to 21:00 h (local time) with 760 SLPM dry air containing 391 µmol mol^{-1} CO_2 at the chamber inlet. The chambers were supplied with CO_2 depleted in ^{13}C ($\delta^{13}C = -48.6‰$) compared to ambient air CO_2 ($\delta^{13}C = -8.5‰$). Each morning at sunrise, each chamber was watered with the equivalent of the previous day's evaporation plus an extra of 20% to account for run-off (5–10 mm in total). Sensors for air temperature/relative humidity and soil temperature (approx. 5 cm depth) were placed inside the OTC, while PPFD sensors were placed outside. The air sampling tubes inside each chamber were installed at 20–25 cm above the canopy.

Nighttime respiration measurements. During darkness (between 23:30 and 5:30 h local time) respired CO_2 was analysed by measuring gas exchange of each OTC, in combination with C isotope analysis of CO_2. For these measurements, the air flow through the chamber was kept at 100 SLPM (compared to 760 SLPM during daytime labelling).

CO_2 concentration at the chamber inlet was maintained at 388 µmol mol^{-1} and $\delta^{13}C$ at −48.6‰ throughout the nighttime respiration measurements, which is the same value as during daytime labelling. To allow for equilibration after reducing the air flow, chambers were flushed at least for one hour before first measurements were taken. The net CO_2 flux, F_{resp}, and the ^{13}C signature of the net flux, δ_{resp}, were calculated from the change in CO_2 concentration and $\delta^{13}C$ between chamber inlet and outlet, according to mass balance equations:

$$F_{resp} = \frac{F_{air}}{V_{mol}\, A_{chamber}}(C_{out} - C_{in}), \tag{2.1}$$

$$\delta_{resp} = \frac{\delta_{out}\, C_{out} - \delta_{in}\, C_{in}}{C_{out} - C_{in}}. \tag{2.2}$$

F_{air} is the air flow through the chamber (corresponding to 100 SLPM), $A_{chamber}$ the chamber base area and V_{mol} the molar volume of gases (22.4 l mol^{-1}). C_{in} and C_{out} are the CO_2 concentrations at chamber inlet and outlet, and δ_{in} and δ_{out} the respective $\delta^{13}C$ values.

The fraction of newly assimilated (labelled) carbon in respired CO_2, f_{new}, was calculated from δ_{resp} according to mass balance considerations as

$$f_{new} = \frac{\delta_{resp} - \delta_{old}}{\delta_{new} - \delta_{old}}. \tag{2.3}$$

δ_{old} and δ_{new} are the ^{13}C signatures of CO_2 respired by the non-labelled ecosystem (measured in the night before the beginning of the labelling experiment), and by the labelled ecosystem at the new isotopic equilibrium. As labelling duration was too short to achieve isotopic equilibrium, δ_{new} was estimated from C isotope discrimination, Δ, and the measured $\delta^{13}C$ of CO_2 inside the OTC during daytime tracer uptake, δ_{out}(daytime), as in Schnyder *et al.* (2003):

$$\delta_{new} = \frac{\delta_{out}(\text{daytime}) - \Delta}{1 + \Delta}. \tag{2.4}$$

Δ was obtained from the measurements of the unlabelled system as:

$$\Delta = \frac{\delta_{amb} - \delta_{old}}{1 + \delta_{old}}, \tag{2.5}$$

with δ_{amb} denoting the C isotope composition of ambient air at the site during daytime hours. This estimation was based on the assumption that discrimination was not altered by the conditions inside the OTC, so that discrimination was the same for the labelled and non-labelled fractions of respired CO_2.

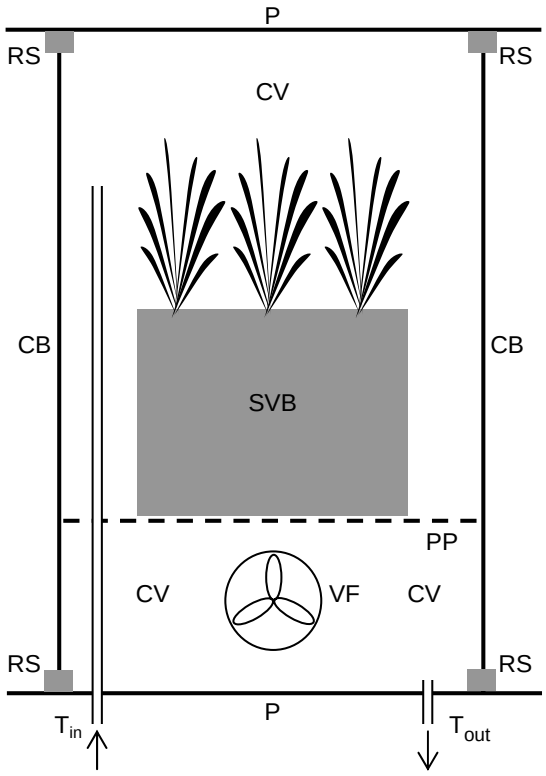

Figure 2.3: Schematic diagram of the laboratory-based open $^{13}CO_2/^{12}CO_2$ gas exchange cuvette, adapted for reference measurements of the isotopic composition of ecosystem respiration. CB, cuvette body (PVC tube, 30 cm height, 19 cm diameter); P, top and bottom plate of cuvette (PVC); RS, rubber sealing; CV, cuvette volume; PP, perforated plate; SVB excised soil+vegetation block; T_{in} and T_{out}, air inlet and outlet tubes; VF, ventilation fan.

Reference measurements. A laboratory-based open $^{13}CO_2/^{12}CO_2$ gas exchange system (Lötscher *et al.*, 2004) was used for reference measurements of the isotopic composition of ecosystem respiration. For that purpose, four soil+vegetation blocks of 15 cm diameter and 10–11 cm soil depth were excised from each labelled site immediately after the termination of labelling and on-site respiration measurements. The laboratory-based system of Lötscher *et al.* (2004) was adapted with a new cuvette (Fig. 2.3). Ecosystem respiration was measured by placing the excised soil+vegetation blocks in the cuvette volume of the system, completely enclosing the block in the cuvette. The four cuvettes (one for each soil+vegetation block) were placed in a plant growth cabinet controlled at 18 °C, the soil temperature of the labelling site at the beginning of the experiment. Cuvettes were operated in the open mode by flushing air through each cuvette, and measuring the concentration and isotopic composition of respired CO_2 in the inlet and outlet air fluxes.

Results

Chamber performance

Mixing of chamber air. The mixing characteristics of OTCs were analysed by following the kinetics of CO_2 concentration change in chamber headspace air following CO_2 concentration switches in the inlet air flow. The increases and decreases of CO_2 concentration in the chamber headspace fitted exponential curves ($r^2 > 0.999$), indicating near-instantaneous mixing of incoming air with chamber headspace air. Half-lives at the different positions in the chamber varied very little, and ranged between 242 and 254 s (Fig. 2.2). The longest half-lives were observed at the chamber bottom, the shortest ones close to the chamber top.

In case of instantanous mixing, the half-life depends only on the rate of air flow through the chamber and the chamber volume. Due to the greenhouse effect, air inside the chamber is heated up, causing thermal expansion of the air volume. With chamber air temperatures of 20–30 °C, the theoretical half-life ranged between 230 and 240 s. The longer half-life at the chamber bottom (compared to the upper chamber section) was related to heating of air between entering the chamber close to the bottom and leaving through the open top.

Ambient air incursion. Chamber designs with and without the plate mounted below the frustrum top of the OTC (RP in Fig. 2.1) were investigated with respect to the effect on air incursion, assessed by the ratio $\mathrm{air_{amb}}/\mathrm{air_{chamber}}$. Other chamber parameters and operating conditions were held the same as during respiration measurements (Table 2.1). CO_2 concentration data were averaged over the half-life of chamber air.

Chamber parameters	v_{exit} ($\mathrm{m\,s^{-1}}$)	0.2
	Air flow (SLPM)	100
	Opening (% of base area)	1
$\mathrm{air_{amb}}/\mathrm{air_{chamber}}$	Chamber without plate	0.065 ± 0.020 ($n = 3$)
	Chamber with plate	0.0018 ± 0.0007 ($n = 71$)
Ratio	(without plate)/(with plate)	37.1

Table 2.1: Comparison of open-top chamber with and without plate mounted at chamber top below the frustrum with respect to ambient air incursion ($\mathrm{air_{amb}}/\mathrm{air_{chamber}}$: ratio of ambient air to total air inside the chamber; mean ± SD of measurements at windspeed between 2 and 4 $\mathrm{m\,s^{-1}}$).

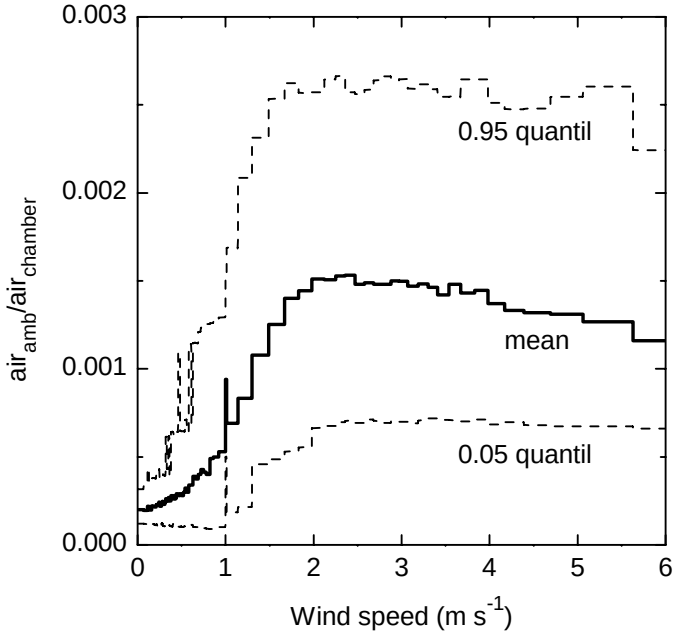

Figure 2.4: Influence of wind speed on the ratio $\mathrm{air_{amb}}/\mathrm{air_{chamber}}$ for the chamber setup used during respiration measurements (opening size 1% of base area; air flow $100\,\mathrm{l\,min^{-1}}$; chamber with removable plate; see Fig. 2.1). Each step represents the mean (solid line) and 0.05 and 0.95 quantil (dashed lines), respectively, of 1000 measurements (1 s averages) falling into the wind speed interval indicated by the width of the horizontal step.

Ambient air incursion into the chamber was reduced nearly by a factor of 40 when the plate was mounted. Thus, the volume between the plate and the frustrum top acted as an effective buffer between the chamber body and ambient air. Accordingly, investigations of the effect of wind speed on ambient air incursion were performed with the plate mounted, as during respiration measurements. On average, $\mathrm{air_{amb}}/\mathrm{air_{chamber}}$ was around 0.0015 for wind speeds above $2\,\mathrm{m\,s^{-1}}$ and lower for lower wind speeds (Fig. 2.4). In 95% of the measurements $\mathrm{air_{amb}}/\mathrm{air_{chamber}}$ was below 0.0026. For wind speeds below $2\,\mathrm{m\,s^{-1}}$ this fraction was even lower (Fig. 2.4).

Disturbance of soil CO_2 efflux. Pressure difference between the outside and inside of the OTC did not increase significantly at exit velocities $v_{\mathrm{exit}} < 0.2\,\mathrm{m\,s^{-1}}$ ($P = 0.16$, Fig. 2.5 a). But, beyond $0.2\,\mathrm{m\,s^{-1}}$ overpressure inside the chamber increased quadratically with increasing v_{exit} (Fig. 2.5 b). Soil CO_2 efflux, observed simultanously with pressure difference, showed also no significant relationship with v_{exit}, if v_{exit} was $< 0.2\,\mathrm{m\,s^{-1}}$ ($P = 0.30$, Fig. 2.5 c). But, soil CO_2 efflux decreased when v_{exit} increased between 0.2 and $2\,\mathrm{m\,s^{-1}}$. Increases of v_{exit} beyond $2\,\mathrm{m\,s^{-1}}$ caused no further decrease of soil CO_2 efflux (Fig. 2.5 d).

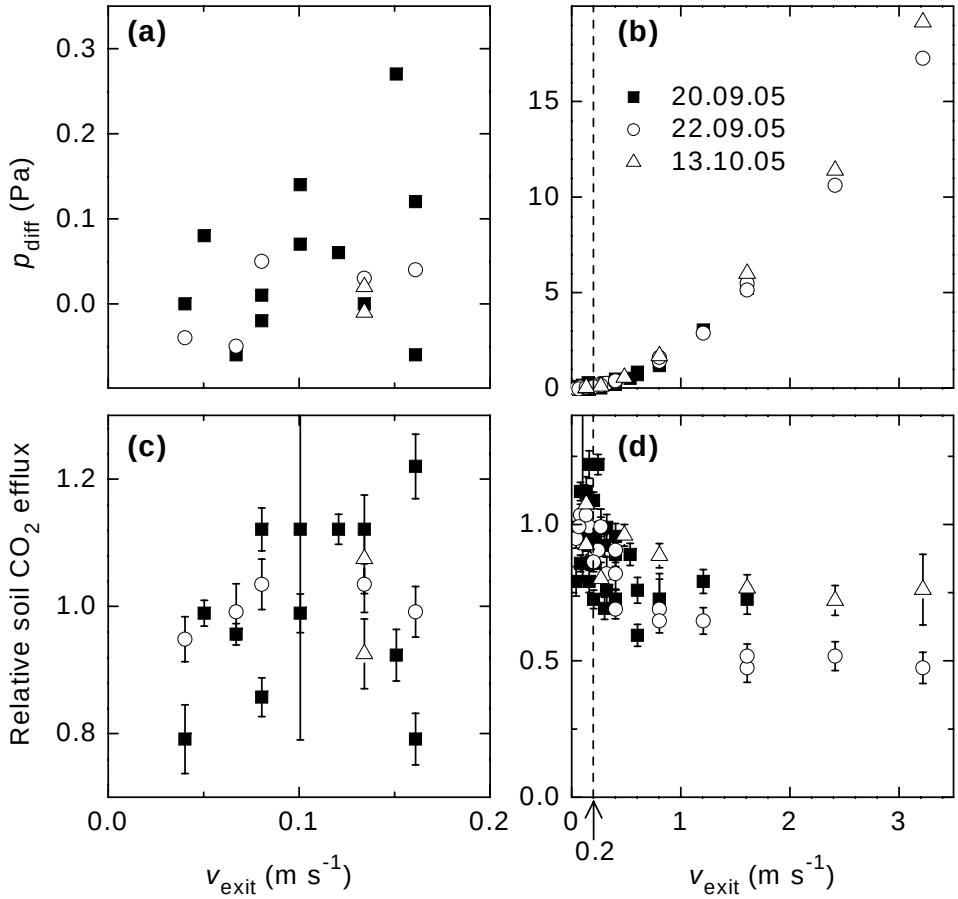

Figure 2.5: (a), (b) Overpressure and (c), (d) relative soil CO_2 efflux observed inside a chamber enclosing a grassland canopy, but with aboveground vegetation clipped and removed. Different symbols indicate different days of observation. Relative soil CO_2 efflux is related to the mean soil CO_2 efflux for $v_{exit} < 0.2\,\mathrm{m\,s^{-1}}$ to facilitate comparison of measurements from different days with different absolute efflux rates. (a) and (c) expand the range of $v_{exit} < 0.2\,\mathrm{m\,s^{-1}}$.

Climatic conditions inside the chambers. Daytime air temperature inside the OTCs was near-identical to ambient air temperature on average over the whole labelling experiment, with a root mean squared difference (RMSE) of 2.7 °C (based on ∼10 min averages, recorded in each of the four OTCs once per hour; Fig. 2.6 a). Nighttime air temperature during respiration measurements was 0.3 °C lower on average inside the chambers than outside, with a RMSE of 1.2 °C. Even on sunny days (Fig. 2.6 c), maximum temperature inside the chambers did not exeed 28 °C while ambient air temperature reached 30 °C.

All the humidity in the chamber air originated from evapotranspiration inside the chamber, as the air entering the chambers was dry. Relative humidity (Fig. 2.6 b) in the chambers

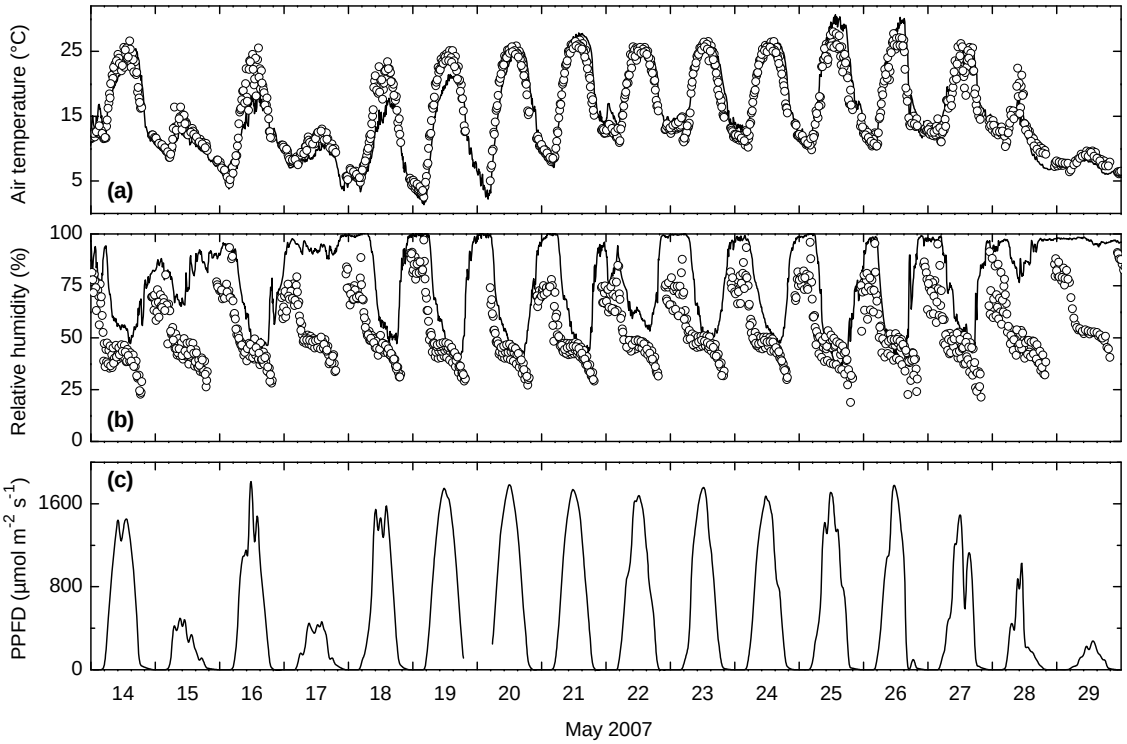

Figure 2.6: (a) Air temperature, (b) relative humiditiy inside (dots) and outside (lines) the chambers and (c) photosynthetic photon flux density (PPFD) outside the chambers during the labelling experiment.

was around 45% during morning, noon and early afternoon, and started to decrease in late afternoon to about 30% at sunset. Outside the chambers relative humidity was lowest at around 15:00 h, with 58% on average. During nighttime respiration measurements, relative humidity in the chambers was 73% on average, compared to 95% outside the chambers.

Overall, the modifications of climatic conditions by the OTCs were quite modest and well inside the range of chamber effects reported by others (e.g. Sanders *et al.*, 1991; Leadley & Drake, 1993; Liu *et al.*, 2000; Dore *et al.*, 2003). This was true except for air humidity which was lower than ambient in the present system, but is higher than ambient in most OTCs (e.g. Dore *et al.*, 2003). Ambient temperature was tracked rather well by the new OTC system.

Concentration and isotope composition of CO_2 during labelling. CO_2 concentration and $\delta^{13}C$ at the chamber inlet and outlet during daytime are shown in Fig. 2.7. As expected, CO_2 concentration at the outlet was lower than at the inlet due to photosynthetic CO_2 uptake, and $\delta^{13}C$ at the outlet was enriched compared to the inlet due to photosyn-

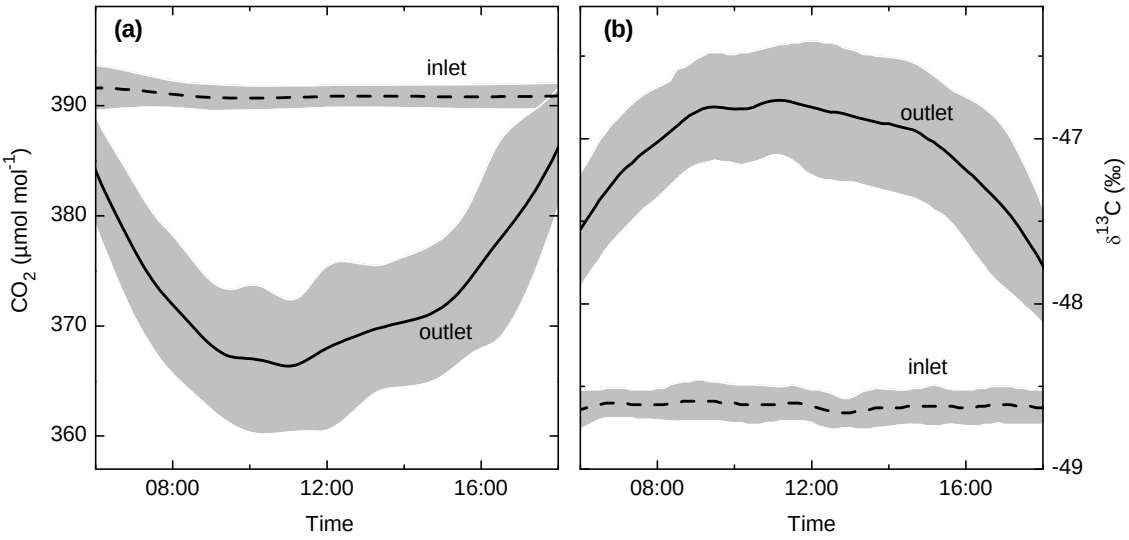

Figure 2.7: Average diurnal cycle of (a) CO_2 concentration and (b) $\delta^{13}C$ of CO_2 in air at chamber inlet (dashed lines) and outlet (solid lines) during the light period. Lines indicate the mean of the four open-top chambers during the two weeks-long labelling experiment, shaded areas indicate SD including day-to-day variation as well as variation between the different chambers.

thetic discrimination against ^{13}C. In chamber air (reflected by the outlet observations), CO_2 concentration was comparable to ambient conditions, with $367 \pm 6.5\,\mu mol\,mol^{-1}$ at noon. $\delta^{13}C$ at the chamber outlet was up to 1‰ more depleted in the morning and evening than during the brightest period of the day. But, as the assimilation rate was lower in the morning and evening, the contribution of these periods with more depleted $\delta^{13}C$ to the total amount of assimilated tracer was small. The assimilation-weighted mean $\delta^{13}C$ of CO_2 in the OTCs was -46.9‰ (while the daytime mean $\delta^{13}C$ of ambient CO_2 was -8.5‰). SD including day-to-day variation as well as variation between the chambers was $1.2\,\mu mol\,mol^{-1}$ and 0.11‰ at the chamber inlet and $6.5\,\mu mol\,mol^{-1}$ and 0.38‰ at the chamber outlet.

Labelling kinetics of ecosystem respired CO_2

The rate of total ecosystem respiration, F_{resp}, measured online in the field, was 6.7 $\pm 0.3\,\mu mol\,m^{-2}\,s^{-1}$ (SE, $n = 68$) on average during the whole labelling experiment. $\delta^{13}C$ of ecosystem respired CO_2 (δ_{resp}) is shown in Fig. 2.8 a. In the unlabelled ecosystem (before the start of labelling), δ_{resp} was -26.7 ± 0.2‰ (SE, $n = 4$). Labelling with ^{13}C-depleted CO_2 caused a decrease of δ_{resp}. This decrease was fast during the first few days of labelling,

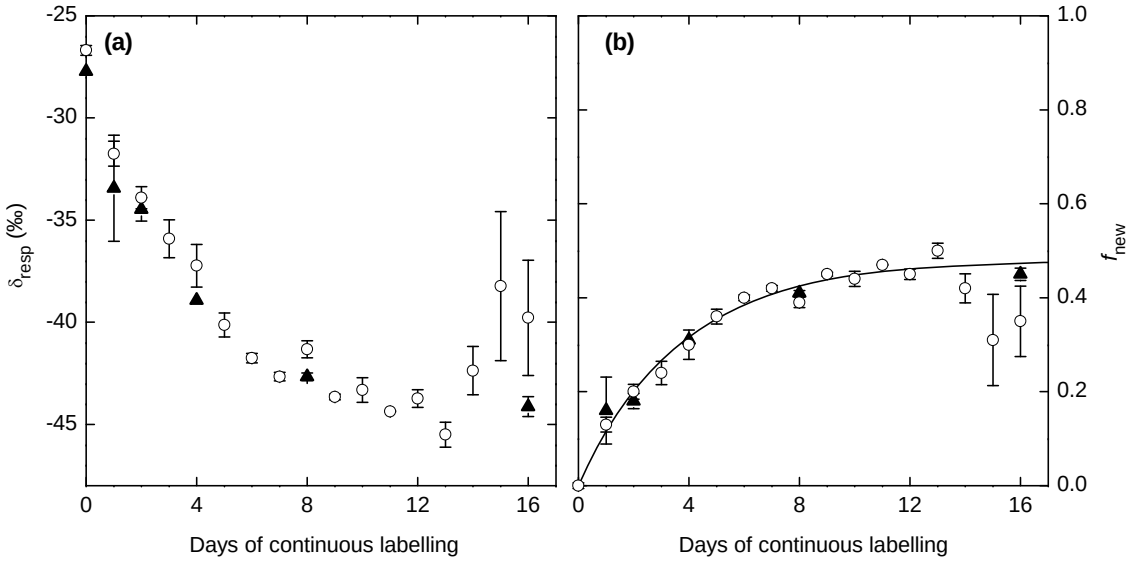

Figure 2.8: Labelling kinetics of ecosystem respired CO_2. (a) $\delta^{13}C$ of ecosystem respiration and (b) fraction of labelled C in ecosystem respired C during a 16 days-long continuous labelling experiment. Respiration measurements were made at night. Open circles indicate online-measurements in the field, closed triangles refer to laboratory-based reference measurements on excised soil+vegetation blocks under controlled conditions. Error bars indicate SE ($n = 2$-9). Line in (b) is the fit according to Eqn. 2.6. Extreme rainfall occurred on days 15 and 16. Data from these days were not included in the fit.

but then slowed until δ_{resp} became almost constant at approx. -44‰ in the second week of labelling. The time-course of δ_{resp} was translated into f_{new}, the fraction of labelled carbon in respired carbon, using Eqns. 2.3 and 2.4 (Fig. 2.8 b) and a Δ of 18.7‰, as determined by gas exchange measurements prior to labelling (Eqn. 2.5).

Reference values of δ_{resp} measured in the laboratory-based gas exchange system tended to be 1–2‰ more depleted than in-situ observed values, independent of the duration of labelling. Translation of δ_{resp} to f_{new} is relative to the unlabelled system for both measurement methods, and so eliminated the offset between laboratory and in-situ measured δ_{resp}. Accordingly, f_{new} from (laboratory) reference and in-situ measurements agreed within measurement uncertainty (Fig. 2.8 b). Extreme rainfall occurred on the last two days of the experiment (approx. $60\,\mathrm{mm\,d^{-1}}$), which caused saturation of soil with water even inside the chambers. Measurements accomplished in that period were 'noisy' and not considered in the following analysis of the labelling kinetics.

The kinetics of f_{new} was approximated ($r^2 = 0.97$) with a two-source model, that included one source which obeyed first order labelling kinetics (source A) and another source which

Fit parameter (Eqn. 2.6)	Fit parameter value (± SE)
a	0.48 ± 0.015
$1 - a$	0.52 ± 0.015
$T_{1/2}$ (d)	2.6 ± 0.2

Table 2.2: Parameters characterising tracer kinetics of ecosystem respired CO_2, observed online in the field.

did not release label during the 14 days-long continuous labelling (source B). This was represented by the following single-exponential function:

$$f_{\text{new}}(t) = a(1 - \mathrm{e}^{-bt}), \tag{2.6}$$

in which t denotes labelling duration. The fit parameter a gives the fractional contribution of source A to total ecosystem respiration, and the (fitted) rate constant b describes the turnover of source A. The fractional contribution of source B to ecosystem respiration is given by $1-a$. Simpler models yielded inferior fits to the f_{new} data, whereas double or even higher exponential functions did not improve the goodness of the fit (data not shown). Thus, Eqn. 2.6 represented the simplest model which contained all essential kinetic features of the supply system feeding ecosystem respiration [in other words, this model contained all necessary and no (statistically) redundant features]. The half-life ($T_{1/2}$) of source A was obtained as $T_{1/2} = (\ln 2)/b$ and was 2.6 d (Table 2.2). The contributions of the two sources to ecosystem respiration were very similar: source A contributed 48% and source B 52%.

Discussion

Labelling performance

The new apparatus provided for a strong, uniform and constant $^{13}CO_2/^{12}CO_2$ labelling signal throughout a 16 days-long labelling experiment of a grassland ecosystem under near-natural environmental conditions: (1) the $\delta^{13}C$ of CO_2 in the OTC was maintained at -46.9‰, $\sim$38‰ less than that of ambient CO_2 with a precision (SD) of 0.4‰ for variations across the labelling experiment duration and all OTCs; (2) CO_2 concentration was maintained at $367 \pm 6.5\,\mu\text{mol}\,\text{mol}^{-1}$ at midday, and (3) mixing of CO_2 inside the OTC was spatially uniform and near-instantaneous.

The small variation in the concentration and isotopic composition of CO_2 supplied to the chambers is a measure of the combined precision of the gas mixing and the measurement device (infrared gas analyser and mass spectrometer) and was within the range reported by Schnyder *et al.* (2004). The considerably higher variation at the chamber outlet was mainly due to variations in assimilation rate. These variations can not be controlled easily by the experimentalist as they depend strongly on incoming radiation, which varies diurnally and with cloudiness. Nevertheless, the variations were small in comparison to the labelling signal, which was ∼100 times larger than the labelling precision, due to the high air flow through the OTCs. Air incursion also contributed to the variations at the chamber outlet, but these variations were negligible compared to the variations caused by assimilation. Furthermore, near-instantanous mixing led to homogeneous tracer distribution inside the chamber. In consequence, sampling of chamber outlet air could be performed anywhere inside the well mixed chamber, since the conditions inside the chamber were uniform.

In-situ observation of tracer kinetics in respired CO_2

The labelling kinetics of respiratory CO_2 was measured accurately and precisely by the OTC-based online $^{13}CO_2/^{12}CO_2$ gas exchange system as confirmed by the reference measurements of f_{new}. In the reference system cuvettes, the excised soil+vegetation blocks were completely enclosed and hence all respired CO_2 was captured by the measurements. The concordance of f_{new} values obtained with both methods provides convincing evidence that the new OTC method captured the unbiased isotopic signal of total ecosystem respiration, despite the fact that the OTCs were open at the bottom. The high accuracy and precision was related to two main features of chamber design and operation conditions: (1) the effective prevention of ambient air incursion into the chamber by the buffered vent of the OTCs, and (2) the absence of pressure effects on soil CO_2 efflux during nighttime respiration measurements. In windy conditions (wind speeds of 2–3 $m\,s^{-1}$ during nighttime measurements), air incursions caused an $air_{amb}/air_{chamber}$ ratio of 0.0015, which meant a change of 0.05‰ of δ_{out}. This effect translated into a 0.5‰ change of δ_{resp} and a 1% decrease of f_{new}. In calm conditions (which prevailed during most nights) less ambient air was blown into the OTCs. Simultaneously, a given amount of ambient air entering the chamber brought a larger quantity of 'contaminating' CO_2, due to the larger nighttime build-up of ambient CO_2 concentration. Nevertheless, the total impact of air incursion on f_{new} was $<1\%$ in calm nights. According to Baldocchi *et al.* (1989) the efficiency of

preventing air incursion into OTCs is dependent on the relationship between chamber volume size and effective eddy size. In the present OTCs the buffer volume had a height of 0.2 m, which suppressed the formation of a roll vortex in the OTCs at the prevailing effective eddy size (0.35 m; calculated according to Baldocchi *et al.*, 1989).

Notably, there was a systematic 1-2‰ offset between δ_{resp} measured in the two gas exchange systems. This offset was related to the fact that δ_{resp} decreased during the course of the night (data not shown) and laboratory-based (reference) measurements were carried out several hours after the on-site measurements. The effect of such changes on the labelling kinetics (i.e. the time course of f_{new}) was eliminated by accounting for the diurnal changes, determining δ_{resp} of the non-labelled ecosystem in the two measurement systems. Other factors affecting the δ-offset between the two systems were not found; cross-calibration of the two systems ensured that δ^{13}C measurements were unbiased.

Estimation of f_{new} was based on the assumption that ^{13}C discrimination during photosynthesis (Δ) was the same inside and outside the OTCs and did not vary over time. Almost certainly, this assumption was not exactly true. However, the sensitivity of f_{new} to variations in Δ was small: a 1‰ increase/decrease in Δ caused a 1% decrease/increase in f_{new}. Measurements of community-level Δ in a large range of weather conditions and soil water availabilities indicated that Δ did not vary by more than $\pm$ 1‰ at the experimental site (Schnyder *et al.*, 2006).

Tracer kinetics reveals two sources supplying respiration

The labelling kinetics showed that ecosystem respiration was fuelled by two distinct sources: one was closely connected with current photosynthetic activity, the other was supplied by substrate that was not labelled within the two weeks-long labelling period. A source is defined here as a cluster of biochemical compounds distributed among different organisms, which exhibited the same (or similar) pattern of tracer incorporation (Lehmeier *et al.*, 2008). Thus, although there was a diversity of metabolic activities in the ecosystem, each (major) activity could be assigned to one of two substrate clusters, which differed in carbon age.

Source A, which was turned over by photosynthesis with a half-life of approx. 2.6 d, must have included most (if not all) of autotrophic respiration. Autotrophic respiration is supplied by non-structural components of plant biomass, which are turned over relatively

rapidly by current photosynthate. In a controlled environment study, Lehmeier *et al.* (2008) found a half-life of about 2 d for the total substrate pool feeding root and shoot respiration of *Lolium perenne*, a main component of the grassland ecosystem. In that study, root and shoot respiration exhibited near-identical labelling kinetics. Moreover, only about 5% of root and shoot respiration was supplied by substrates older than 10 d, showing that long-term reserves/storage pools were relatively unimportant substrates of autotrophic respiration. In another study with the same species, 50% of the root exudates were turned over by current photosynthate within 4.5 d (Thornton *et al.*, 2004). In addition, it has been shown that arbuscular mycorrhizal mycelia can provide a fast pathway for respiratory release of current photosynthate, releasing C within hours to days after its assimilation under field conditions (Johnson *et al.*, 2002; see also Heinemeyer *et al.*, 2006; Hawkes *et al.*, 2008). Furthermore the observed half-life of source A compares reasonably well with the mean age of 5–8 d (corresponding to a half-life of 3.5–5.5 d), determined for autotrophically respired C, including respiration from root-associated microbes, in a California mountain grassland ecosystem (Carbone & Trumbore, 2007). All these components (shoot, root and rhizosphere respiration) must have contributed to the respiratory activity associated with source A, and the sum of these activities constitutes autotrophic respiration (Hanson *et al.*, 2000; Subke *et al.*, 2006; Trumbore, 2006; but see also Chapin *et al.*, 2006; Kuzyakov, 2006). Therefore, we regard the total activity of source A (about half of ecosystem respiration) as a measure of autrotrophic respiration.

The other source (source B) did not release any label within the two weeks-long labelling period, showing that it was supplied by pools with very slow turnover ($\geq$ months) or that the release of the substrate from the pools occurred only after an extensive lag (delay). Leaf and root litter are the main substrates for heterotrophic respiration (Ryan & Law, 2005), as structural biomass is the C source for the various heterotrophic pathways including decomposition via soil organic carbon. C incorporated into structural biomass of leaf and root tissues is protected from respiratory consumption until the end of the tissues' life span, when it passes on to the litter fraction and becomes available for decomposers. Leaf life span of the dominant species at the study site was approximately 27 d (I. Schleip, unpublished data). Others have observed leaf life spans of 22–95 d in a range of grassland species and sites (Diemer *et al.*, 1992; Lemaire & Chapman, 1996; Ryser & Urbas, 2000). The life span of grass roots is even longer, in the order of months (Van der Krift & Berendse, 2002). Thus, all in all, only a very small amount of labelled plant material had been turned into litter and soil organic matter during the labelling experiment. Therefore,

all (heterotrophic) processes decomposing old (non-labelled) dead plant material and soil organic matter were pooled in source B. Resolving further functional components of source B would require extension of the labelling duration.

In conclusion, this work presents a new OTC-based continuous $^{13}CO_2/^{12}CO_2$ labelling and gas exchange measurement system for studies of C allocation and turnover of grassland ecosystems, including the assessment of respiratory substrate pool kinetics. Tests of chamber performance and optimization of OTC design and operation conditions minimised common artefacts such as ambient air incursion and suppression of soil CO_2 efflux, and ensured a high accuracy and precision of daytime $^{13}CO_2/^{12}CO_2$ labelling and nighttime respiration measurements. The method is well suited for labelling studies at any CO_2 concentration level, from subambient to elevated CO_2, as was also demonstrated by Lehmeier *et al.* (2005) in a controlled environment system employing the same gas exchange and labelling methodology. We suggest that the two kinetically distinct sources of respiration detected in this work at ambient CO_2 concentration represent the autotrophic (including rhizosphere) and heterotrophic components of grassland ecosystem respiration.

3 Non-steady-states of the soil CO_2 pool affect measurements of soil respiration: A quantitative investigation of the underlying mechanisms

Summary

The isotopic composition of soil respiration is usually assessed by measuring the isotopic composition of CO_2 emerging from the soil. The latter can differ significantly from the CO_2 actually produced by respiration in the soil due to non-steady-states of the soil CO_2 pool through which the respiratory CO_2 must pass before it emerges into the atmosphere. This divergence (termed 'bias' in the following) can result from natural causes, but is probably most common in CO_2 tracer studies.

We performed a quantitative analysis of mechanisms which can underlie such biases with a soil CO_2 transport model. It accounted for diffusion of $^{12}CO_2$ and $^{13}CO_2$ in the soil, dissolution of CO_2 in soil water and mass displacement of soil air. Model predictions and observations of CO_2 accumulating in closed chambers were investigated in an ecosystem which was labelled with $\sim$40‰ depleted CO_2. The 'true' isotopic composition of ecosystem respiration was derived from independent steady-state open chamber measurements.

The observed isotopic composition of CO_2 emerging from the soil was depleted by an additional 11.2‰ relative to ecosystem respiration in the labelled ecosystem due to non-steady-state effects, but there was no difference in a non-labelled ecosystem. Similarly, model predictions were biased by -9.2‰ on average, if three mechanisms were considered: (1) the change of the concentration and isotopic composition of chamber air CO_2 during measurements, (2) the dissolution of labelling CO_2 in soil water, and (3) the displacement

of soil air during daytime tracer application. All three processes contributed significantly to the observed bias.

The mechanisms affecting the isotopic composition of soil CO_2 efflux and enlargement of the soil CO_2 pool by exchange of CO_2 between water and air pores are potentially relevant to various investigations of soil and ecosystem respiration isotopic composition, including free air carbon dioxide enrichment (FACE) experiments and application of common chamber techniques under natural conditions.

Introduction

The isotopic composition of soil respiration contains information about the processes involved in ecosystem carbon(C) cycling (e.g. Amundson *et al.*, 1998; Andrews *et al.*, 1999; Cisneros-Dozal *et al.*, 2006; Hahn *et al.*, 2006; Taneva *et al.*, 2006). To reveal this information, the isotopic signal of respiration needs to be measured accurately, ideally by sampling CO_2 directly and instantanously at the site of respiratory production (hereafter referred to as 'respiratory CO_2 production'). As soil respiratory CO_2 production is dispersed belowground, it is commonly assessed by measuring CO_2 which emerges from the soil surface into the overlying atmosphere (hereafter referred to as 'soil CO_2 efflux'). On its way, the respired CO_2 passes through the soil CO_2 pool by diffusion and thereby mixes with CO_2 in the soil pores. Hence, soil CO_2 efflux can differ isotopically from respiratory CO_2 production due to non-steady-states of the soil CO_2 pool. This divergence is termed 'bias' in the following. It is expected to confound observation of the isotopic composition of soil respiration on timescales ranging from short-term over diurnal to synoptic, as it takes hours to days of respiratory CO_2 production to generate the amount of CO_2 stored in soil air pores and days to weeks to generate the total amount of CO_2 stored in soil pores including CO_2 dissolved in soil water.

CO_2 concentration and isotopic composition in soil air pores are commonly described by respiratory CO_2 production and diffusive exchange (e.g. Cerling, 1984), treating $^{12}CO_2$ and $^{13}CO_2$ as separate diffusing gases and taking into account their different diffusivities. This approach has been successfully applied to predict deviations from the steady-state (Nickerson & Risk, 2009a,b,c; Subke *et al.*, 2009). Nickerson & Risk (2009b) investigated the application of a 2-component mixing approach (Keeling, 1958) to CO_2 accumulation in the headspace of a closed soil respiration chamber. In this approach the increase of CO_2

concentration and changes in its isotopic composition were attributed to the enclosed respiratory source. Under the assumption that the isotopic signature of the respiratory source is constant, plotting the isotopic composition vs. the inverse concentration in the mixture, the so-called Keeling plot, leads to a straight line. The intercept represents the isotopic signature of the source. Nickerson & Risk showed that the isotopic composition of the soil CO_2 efflux changes during CO_2 accumulation, violating the constant source assumption. This deviation of the Keeling plot from linearity caused Keeling plot intercepts to differ up to 4‰ from the actual isotopic composition of respiratory CO_2 production. Theoretically, other chamber approaches were expected to cause even larger biases (Nickerson & Risk, 2009c).

The amount of CO_2 dissolved in soil water can be much larger (up to 100 times) than that in soil air pores, and can slow the equilibration between respiratory CO_2 produced throughout the soil and soil CO_2 efflux. Thus, dissolved CO_2 has the potential to amplify the bias by retarding the equilibration. The extent of the contribution from this extended soil CO_2 storage pool depends on the equilibration time between CO_2 in soil air and dissolved in soil water (including CO_2 dissolved in water, carbonic acid, bicarbonate and carbonate): when this equilibration occurs fast compared to the time that CO_2 stays in soil air pores, then the total soil CO_2 pool (gaseous + dissolved CO_2) is involved in non-steady-state effects.

Mass flow influences the distribution of CO_2 within soil pores by displacing soil air masses and thus the soil CO_2 efflux. This can occur for example when a chamber is placed on soil. Even small pressure differences between chamber inside and outside, in the order of 1 Pa, have been shown to considerably influence the soil CO_2 efflux (Fang & Moncrieff, 1998; Lund *et al.*, 1999) by causing advection (Kanemasu *et al.*, 1974). To our knowledge, the influence of mass flow on measurements of isotopic composition of soil respiration and the impact of the increased soil CO_2 pool due to dissolution on non-steady-state effects have not yet been quantified.

$^{13}CO_2/^{12}CO_2$ labelling experiments cause strong isotopic disequilibria between soil air CO_2 and the overlying atmosphere. Subke *et al.* (2009) showed that a pulse change in the isotopic composition of atmospheric CO_2 was accompanied by a change in the isotopic composition of CO_2 in soil pores, due to diffusion of the tracer into the soil pore space. Back diffusion of the tracer stored in the soil pores into the atmosphere during label chasing resulted in observation of an abiotic tracer flux (non-biological tracer flux from

the soil into the overlying atmosphere, caused by physical processes but not by respiration of previously assimilated labelled C) for up to 2 d after exposure to the tracer. In pulse labelling experiments, the labelling CO_2 is usually highly enriched in $^{13}CO_2$, causing a strong isotopic gradient between CO_2 in soil air pores and overlying atmosphere, which drives the diffusive flux. Tracer diffusion into the soil under such conditions was also noted by Staddon *et al.* (2003) and Leake *et al.* (2006). In continuous labelling experiments, including FACE (free air carbon dioxide enrichment) experiments, the change in isotopic composition is much smaller (e.g. Nitschelm *et al.*, 1997; Matamala *et al.*, 2003; Asshoff *et al.*, 2006; Keel *et al.*, 2006; Pregitzer *et al.*, 2006; Taneva *et al.*, 2006) and maintained over long periods. But the potential of such a change to cause abiotic tracer fluxes has not yet been investigated under these conditions.

In a continuous labelling experiment investigating substrate supply of ecosystem respiration in a temperate grassland ecosystem under field conditions (Gamnitzer *et al.*, 2009), we found indications for discrepancies between isotopic composition of respiratory CO_2 production and that of soil CO_2 efflux. Large deviations were observed for isotopic signatures of ecosystem respiration measured in closed chambers compared to that measured in steady-state open chambers, validated by an independent laboratory-based method to represent respiratory CO_2 production. Here we quantitatively analyse mechanisms potentially causing such discrepancies between results from different methods. For this purpose, we established a soil CO_2 transport model which accounted for diffusion of $^{12}CO_2$ and $^{13}CO_2$, dissolution of CO_2 in soil water and mass flow of soil air. This model was applied to study abiotically-driven fluxes of the tracer. We simulated the labelling experiment and predicted Keeling plot intercepts derived from CO_2 accumulation in closed chambers during the time course of labelling. Simulation results were compared to observations to clarify the mechanisms which underlie the observed bias. Finally, consequences of these mechanisms for commonly applied isotopic approaches are discussed.

Material and Methods

Field labelling experiment

In a $^{13}C/^{12}C$ labelling experiment, described in detail by Gamnitzer *et al.* (2009), a temperate grassland ecosystem at Grünschwaige Grassland Research Station (Schnyder *et al.*, 2006) was continuously labelled for 2 weeks, using an open-top chamber system. The label was applied during daytime hours by altering the isotopic composition of CO_2 in the chamber headspace air, while CO_2 concentration was similar to ambient CO_2 concentration. During nighttime hours, ecosystem respiration was measured online in the field using two different approaches: (1) respiration measurements in each night started after sunset with closed chamber measurements (see below; more exactly termed non-steady-state non-flow-through system, Livingston & Hutchinson 1995), lasting approx. until midnight; and subsequently (2) open chamber respiration measurements (Gamnitzer *et al.* 2009; more exactly termed steady-state flow-through system, Livingston & Hutchinson 1995) were conducted from midnight until sunrise (Fig. 3.1). In both approaches, CO_2 concentration and isotopic composition were analysed online with an infrared gas analyser (LI 7000; Li-Cor, Lincoln, NE, USA) and a continuous-flow isotope-ratio mass spectrometer (Delta Plus Advantage; Thermo Electron, Bremen, Germany) interfaced with a gas chromatic column (Gasbench II; Thermo Electron, Bremen, Germany) (Schnyder *et al.*, 2004). Carbon isotopic compositions are presented as $\delta^{13}C = R_{sample}/R_{standard} - 1$, where R_{sample} and $R_{standard}$ are the $^{13}C/^{12}C$ ratios in the sample and in the international VPDB standard. Measurements were corrected for linearity effects (i.e. dependence of the raw $\delta^{13}C$ value on the actual CO_2 concentration). $\delta^{13}C$ of the labelling CO_2, to which the plants were exposed, was $-46.9‰$.

Closed chamber approach to measure ecosystem respiration

For the closed chamber respiration measurements, the chamber air supply was disconnected and the chamber top was closed with a lid. CO_2 concentration and isotopic composition were monitored subsequent to chamber closure by analysing 6 consecutive samples (1 sample every 120 s) within a 15-min measurement cycle. Sample air was drawn continuously from the chamber headspace to the analysers at approx. 1.6 standard litres per minute. The chamber was not sealed tightly to allow for replacement of the air re-

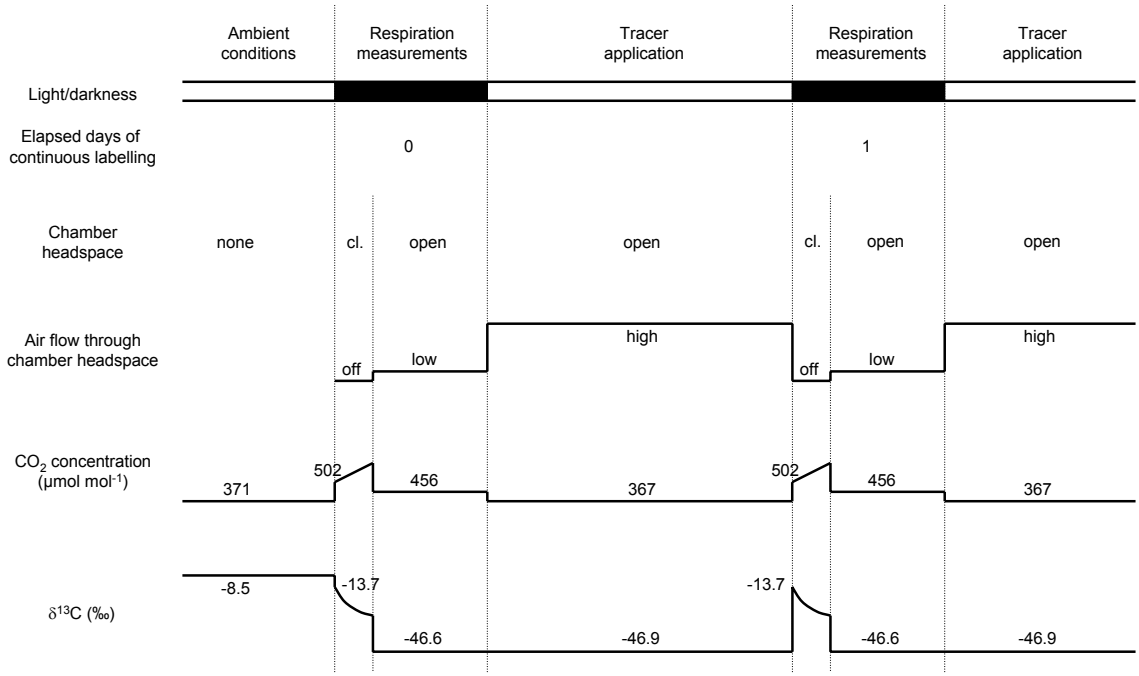

Figure 3.1: Schematic sequence of labelling experiment, including chamber headspace conditions (cl.: closed) of air flow, CO_2 concentration and isotopic composition. Concentration and $\delta^{13}C$ values are averages observed during the labelling experiment and were used as input parameters in the model simulation. For closed chamber headspace, values are given at chamber closure.

moved for sampling by ambient air entering through vents in the chamber. The chamber was lifted and replaced in its original position immediately before the closed chamber measurement started, substituting the labelling air in the chamber headspace (from the preceding labelling day) with ambient air. This was done to adapt initial conditions for closed chamber measurements in the labelled ecosystem to those in the unlabelled control measurements. Furthermore, this ensured that air drawn into the chamber to replace sampled air was identical to the background signal in the chamber headspace air and thus diluted the respiratory signal, but had no effect on the Keeling plot intercept.

From the time course of the CO_2 increase, the net CO_2 flux of total ecosystem respiration into the chamber air, F_{resp}, was calculated as

$$F_{\mathrm{resp}} = \frac{\Delta C}{\Delta t} \cdot \frac{V_{\mathrm{chamber}}}{V_{\mathrm{mol}}\, A_{\mathrm{chamber}}}, \tag{3.1}$$

where ΔC is the CO_2 concentration increase in the chamber headspace during the time interval Δt, V_{chamber} the chamber volume (660 l), A_{chamber} the chamber base area ($0.83\,\mathrm{m}^2$) and V_{mol} the molar volume of an ideal gas ($22.4\,\mathrm{l\,mol}^{-1}$ at standard conditions; adapted

to site conditions for temperature and pressure). Average respiration rate during the labelling experiment was 6.6 µmol m^{-2} s^{-1}, in agreement with open chamber measurements (Gamnitzer *et al.*, 2009). $\delta^{13}C$ of respiration was determinded following the approach of Keeling (1958). The 6 samples analysed in the 15-min measurement cycle following chamber closure were pooled in one Keeling plot, resulting in an intercept reflecting $\delta^{13}C$ of soil CO_2 efflux.

Soil CO_2 transport model

The movement of CO_2 in soil pore spaces and exchange with the overlying atmosphere was simulated with a vertical transport model, similar to the soil diffusion model of Nickerson & Risk (2009a), but extended to account for dissolution of CO_2 in soil water and vertical displacement of air masses. This was based on the one-dimensional diffusion equation (see e.g. Penman, 1940; Rolston, 1986; Amundson *et al.*, 1998)

$$\frac{\partial C}{\partial t} = \frac{D_{\text{soil}}}{\varepsilon_{\text{air}}} \cdot \frac{\partial^2 C}{\partial z^2} + P, \tag{3.2}$$

where C is the CO_2 concentration in air-filled soil pores, D_{soil} the diffusion coefficient for CO_2 in soil, ε_{air} the air-filled porosity of the soil, P the CO_2 concentration change per unit time in the soil air pores due to respiratory CO_2 production in soil. D_{soil} was derived from D_{air}, the diffusion coefficient for CO_2 in air, according to Millington (1959). Temperature dependence of D_{air} was calculated following Campbell & Norman (1998). t denotes the time and z the depth below the soil surface. For numerical solution of the diffusion equation, the soil was divided into n horizontal layers of thickness $z = L/n$, where L is the thickness of the total soil layer. An additional top layer (depth 0) represents the air above the soil. For each timestep (Δt), the CO_2 concentration change (ΔC) in each layer was calculated as

$$\Delta C(z,t) = \frac{D_{\text{soil}}}{\varepsilon_{\text{air}}} \cdot \frac{C(z+\Delta z,t) - C(z,t)}{\Delta z^2} \cdot \Delta t + \frac{D_{\text{soil}}}{\varepsilon_{\text{air}}} \cdot \frac{C(z-\Delta z,t) - C(z,t)}{\Delta z^2} \cdot \Delta t + P(z) \cdot \Delta t. \tag{3.3}$$

ΔC was determined by the diffusive fluxes into/out of that layer from/to the layer below/above during timestep Δt (according to Fick's second law) and the production in the layer at depth z during the timestep Δt. In the bottom layer (depth L), the diffusive exchange occured only with the layer above. Treatment of the top layer depended on the simulated situation (ambient conditions, open or closed chamber), see 'Simulation runs' below.

The model was adapted to consider dissolution of CO_2 in soil water by partitioning the net amount of CO_2 added to (or removed from) each layer, ΔC, during timestep Δt into a gaseous (N_{air}, amount of C as CO_2 in the gas phase) and a dissolved (N_{water}, amount of C dissolved in the aqueous phase including carbonic acid, hydrogen carbonate and carbonate) fraction. Assuming instantaneous equilibration between the gaseous and the dissolved phase, the concentration in the layer at depth z after the timestep Δt, $C(z, t+\Delta t)$, was given by the concentration in that layer before the timestep, $C(z, t)$, plus the concentration change ΔC multiplied with the fraction of C as CO_2 in the gas phase, $N_{\text{air}}/(N_{\text{air}}+N_{\text{water}})$:

$$C(z, t+\Delta t) = C(z, t) + \frac{N_{\text{air}}}{N_{\text{air}} + N_{\text{water}}} \cdot \Delta C(z, t). \tag{3.4}$$

The ratio of the amount of CO_2 dissolved in soil water pores to the amount of CO_2 in soil air pores, $N_{\text{water}}/N_{\text{air}}$, was derived from dissolution equilibrium as

$$\frac{N_{\text{water}}}{N_{\text{air}}} = 22.4\, K_0 \left(1 + \frac{K_1}{[\text{H}^+]} \left(1 + \frac{K_2}{[\text{H}^+]}\right)\right) \cdot \frac{\varepsilon_{\text{water}}}{\varepsilon_{\text{air}}}. \tag{3.5}$$

K_0, K_1, K_2 are the equilibrium constants for formation of carbonic acid when CO_2 is dissolved in water and dissociates to hydrogen carbonate and carbonate, respectively, and were derived from temperature (Harned & Scholes, 1941; Harned & Davis, 1943). $[\text{H}^+]$ is the concentration of protons, derived from pH. $\varepsilon_{\text{water}}$ and ε_{air} are the water-filled and air-filled soil porosities.

Downwards displacement of air in soil pores (due to increased pressure in the air above the soil) was taken into account by shifting $C(z, t)$ downwards by $\Delta z_{\text{displace}}$ in each timestep Δt, resulting in a concentration change $\Delta C_{\text{displace}}$ due to mixing between the two adjacent layers:

$$\Delta C_{\text{displace}} = \frac{\Delta z_{\text{displace}}}{\Delta z}(C(z-\Delta z, t) - C(z, t)). \tag{3.6}$$

$\Delta C_{\text{displace}}$ was then partitioned in a gaseous and a dissolved fraction according to Eqn. 3.5.

Isotopologues of CO_2 were treated as separate diffusing gases by setting up two sets of equations, one for $^{12}CO_2$ and one for $^{13}CO_2$. Thus, the total CO_2 concentration C and the isotopic signature δ^{13}C could be calculated from $^{12}CO_2$ and $^{13}CO_2$ concentration for each depth layer and each timestep. Fractionation during diffusion was taken into account by applying different diffusivities for the different isotopes: $D_{\text{soil}}(^{12}CO_2)/D_{\text{soil}}(^{13}CO_2) = 1.0044$. Fractionation during dissolution was taken into account by applying different factors $N_{\text{water}}/N_{\text{air}}$ for $^{12}CO_2$ and $^{13}CO_2$ (Thode *et al.*, 1965; Vogel *et al.*, 1970; Mook *et al.*, 1974).

Simulation runs

Step changes in δ^{13}C of the air layer CO_2. The model was used to simulate the effect of step changes in the isotopic composition of CO_2 in the air layer above the soil on the δ^{13}C of soil CO_2 efflux. For that purpose the air layer was maintained constant at ambient conditions, and the model was run until soil air CO_2 reached steady-state. Then δ^{13}C in the air layer was changed to labelling conditions, while all other parameters (including δ^{13}C of respiratory CO_2 production) remained unchanged. When the new equilibrium was reached, δ^{13}C in the air layer was changed back to ambient conditions. Model input parameters characterising conditions for CO_2 transport in the soil were determined for the field site (Table 3.1). The soil layer of thickness $L = 25\,\text{cm}$ was divided into 125 layers of thickness $z = 2\,\text{mm}$. The timestep Δt was set to 12 s for most model runs, and decreased to 3 s or 1 s in case a numerical overflow occurred for $t = 12\,\text{s}$. For some model runs dissolution of CO_2 in soil water was disregarded by setting the fraction of C as CO_2 in the gas phase, $N_{\text{air}}/(N_{\text{air}} + N_{\text{water}})$, to 1. Finally, soil CO_2 efflux was derived from the model according to Fick's first law:

$$\text{efflux}(t) = \frac{D_{\text{soil}}}{V_{\text{mol}}} \cdot \frac{\Delta C_{\text{surface}}(t)}{\Delta z}, \tag{3.7}$$

where $\Delta C_{\text{surface}}$ is the concentration difference at the soil surface (between the air pores of the uppermost soil layer and the overlying atmosphere). δ^{13}C of the soil CO_2 efflux was derived from the simulated $^{12}CO_2$ and $^{13}CO_2$ effluxes.

Labelling experiment and chamber-based respiration measurements. To simulate CO_2 concentration and δ^{13}C in soil air pores below the chamber during the labelling experiment (Fig. 3.1), boundary conditions for the air layer were chosen according to the respective chamber mode. First, the model was run under ambient conditions until soil profiles of CO_2 and δ^{13}C reached steady-state. Then, closed chamber measurements of the respiration signal of the unlabelled ecosystem (control) were simulated by replacing the air layer above the soil by the chamber headspace volume, in which soil CO_2 efflux and shoot respired CO_2 accumulated. Analogous to Keeling plot sampling during the field measurements, 6 consecutive values of simulated air layer CO_2 concentration and δ^{13}C in 2 min intervals were pooled to generate a Keeling plot. Subsequently, conditions during open chamber measurements were simulated by forcing CO_2 concentration and δ^{13}C in the air above the soil to be constant for 7 h (fraction of the dark period not covered by closed

Parameter	Value	Range	Method of determination
Porosity:			estimated from measured wet and dry
total	0.57	0.56–0.58	mass of a defined volume of bulk soil
air-filled	0.25	0.23–0.27	(mean of the top 10 cm of the soil layer)
			and an assumed density of 2.5 g cm^{-3}
			for solid matter
CO_2 production in soil:			
production rate (µmol m^{-2} s^{-1})	5.0	4.0–6.0	determined from observed respiration
			rate (Gamnitzer *et al.*, 2009)
fraction produced in the	0.8	0.5–0.9	exponential distribution with depth,
top 5 cm			adapted to root mass distribution
			(Klapp, 1971)
Temperature (°C)	16.5	10–24	observed soil temperature (5 cm depth)
pH	7.5	7.2–7.8	K. Auerswald, unpublished data
Displacement:			see Section 'Simulation runs'
$\Delta z_{\mathrm{displace}}/\Delta t$ (mm min^{-1})			
dissolution considered	0	2.4	
dissolution disregarded	0	5.3	

Table 3.1: Parameters characterising conditions for CO_2 transport in the soil at the field site.

chamber simulations). Then, a daytime labelling period of 16 h followed: CO_2 concentration and $\delta^{13}C$ in the air layer were again kept constant, and the isotopic signature of respiratory CO_2 production was adapted to include a fractional contribution of labelled C. The latter was derived from the time course of tracer in ecosystem respired CO_2 (respiratory tracer kinetics) observed in open chamber measurements (Gamnitzer *et al.*, 2009). These measurements had been confirmed by an independent method where excised soil+vegetation blocks were completely enclosed in laboratory-based open $^{13}CO_2/^{12}CO_2$ gas exchange cuvettes, and thus represented the 'true' $\delta^{13}C$ of respiratory CO_2 production.

Three respiratory sources were distinguished. One source constituted decomposition of soil organic matter. It was located in the soil, did not respire any tracer and contributed approx. half of the ecosystem respiration. Of the other two sources, one reflected aboveground autotrophic respiration and the other reflected belowground autotrophic respiration. Both supplied recently assimilated C from a pool turned over with a half-life of 2.6 d, and each was assumed to contribute between 20 and 80% of this recently assimilated C pool. The cycle of modelling nighttime measurements in closed and open chamber measurements and daytime labelling was repeated, with increasing amount of label in CO_2 produced by

respiration from day to day, to simulate the 2 week-long continuous labelling experiment.

To investigate model sensitivity, simulation runs were performed by varying individual input parameters within the ranges given in Table 3.1. These ranges represented the uncertainty in determination of the input parameters. The displacement $\Delta z_{\mathrm{displace}}/\Delta t$ was estimated such that the model resulted in a 40% decrease in ecosystem CO_2 efflux. This decrease was observed in measurements of F_{resp} in labelled ecosystem plots (which were exposed to increased pressure during the preceding labelling period, see Gamnitzer *et al.* 2009) compared to control plots (which were not pressurised prior to the measurements; $P < 0.001$). The above-mentioned procedure resulted in $\Delta z_{\mathrm{displace}}/\Delta t$ values of $2.4\,\mathrm{mm\,min^{-1}}$ when dissolution of CO_2 in soil water was considered and $5.3\,\mathrm{mm\,min^{-1}}$ when dissolution was disregarded, respectively. Along with lower F_{resp} in labelled plots than in unlabelled plots, temperature during respiration measurements was also lower (U. Gamnitzer, unpublished data). But the effects of decreasing temperature on respiratory CO_2 production and of displacement on soil CO_2 efflux could not be clearly separated. Thus, the above estimates of $\Delta z_{\mathrm{displace}}/\Delta t$ represented an upper limit for the displacement values. Moreover, lateral diffusion was negligible in the present study according to the requirements provided by Nickerson & Risk (2009b,c) on soil diffusivity, air-filled porosity and chamber deployment time. This is furthermore supported by the fact that the chamber used here was about 10 times larger in diameter than the one studied by Nickerson & Risk.

Results

Simulation of CO_2 in soil air

The modelled depth profiles for CO_2 concentrations and isotopic compositions, calculated with the air layer set to ambient conditions, showed the expected behavior (Fig. 3.2): CO_2 concentration increased with depth from $371\,\mu\mathrm{mol\,mol^{-1}}$ in the overlying atmosphere to $6000\text{–}17000\,\mu\mathrm{mol\,mol^{-1}}$ at the bottom of the soil layer (Fig. 3.2 a). $\delta^{13}C$ changed continuously from $-8.5‰$ in the atmospheric layer to values between $-21.5‰$ and $-22.1‰$ in the bottom soil layer (Fig. 3.2 b). Most of this change occurred in the upper 5 cm of the soil. Compared to $\delta^{13}C$ of CO_2 produced by respiration in the soil, $\delta^{13}C$ in soil air CO_2 was slightly more enriched than the theoretical 4.4‰ (Cerling, 1984), due to ex-

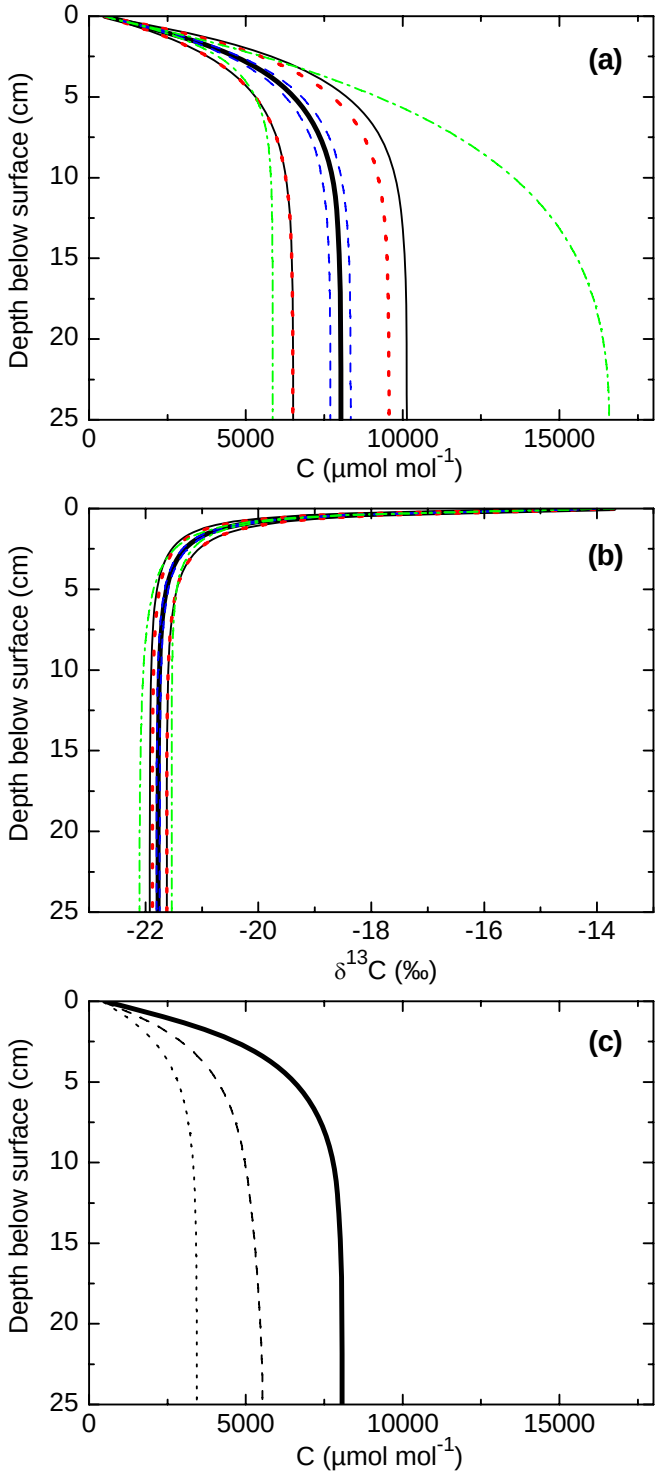

Figure 3.2: Modelled depth profiles of soil air CO_2 concentration and isotopic compositions. (a) concentration and (b) $\delta^{13}C$ under ambient conditions (the beginning of the labelling experiment) for soil conditions observed at the experimental field site (thick black line). Sensitivity of the modelled CO_2 concentration and $\delta^{13}C$ to variations in input parameters within the observed range (Table 3.1) is indicated by the thin lines: variation in soil respiration rate (red dotted), depth distribution of CO_2 production in soil (green dashed-dotted), soil porosity (black solid) and temperature (blue dashed). (c) Influence of downward displacement of soil air masses during daytime tracer application on soil air CO_2 concentration. Simulated soil air CO_2 concentration at the end of a 14 d labelling experiment for the maximum displacement $\Delta z_{\mathrm{displace}}/\Delta t$ (see Table 3.1) when dissolution of CO_2 in soil water is considered (dashed) and disregarded (dotted) in comparison to none displacement (thick).

change with the overlying atmosphere. Sensitivity of modelled profiles to uncertainties in input parameters was smallest for temperature, with changes of soil air CO_2 concentration within 340 µmol mol^{-1} and changes in $\delta^{13}C$ within 0.15‰. Sensitivity was largest for the depth distribution of CO_2 production in the soil: up to a doubling of CO_2 concentration was predicted. In contrast, $\delta^{13}C$ varied very little (within 0.33‰). When dissolution was taken into account, 9 to 32 times the amount of CO_2 in soil air was stored in soil water while CO_2 concentration and isotopic composition in soil air remained unchanged. During the course of the labelling experiment, downward displacement during daytime tracer application shifted the simulated CO_2 concentration profile to smaller values (Fig. 3.2 c). The CO_2 concentration in the deeper soil layers was decreased by 40% when dissolution of CO_2 in soil water was disregarded and 60% when dissolution was considered.

All selected input parameter values provided realistic depth profiles of CO_2 concentration and $\delta^{13}C$. The gradient of both profiles was large in the top centimeters of the soil layer and decreased rapidly with depth. 80% of the soil respired CO_2 was produced in the top 5 cm (Table 3.1). So the main changes occurred above the soil collar depth of 12 cm (compared to a soil layer thickness of 25 cm), confirming the simplified representation of the movement of CO_2 in soil in a one-dimensional model.

Simulation of step changes in isotopic composition of air

A simulated step change in $\delta^{13}C$ in the air layer from −8.5‰ (ambient conditions) to −46.9‰ (labelling conditions) caused model predicted $\delta^{13}C$ of soil CO_2 efflux to become 29.4‰ enriched relative to respiratory CO_2 production (Fig. 3.3 a). Following the change, $\delta^{13}C$ of soil CO_2 efflux decreased asymptotically towards the steady-state value of −26.7‰, which was determined by respiratory CO_2 production. 1 h after the switch, $\delta^{13}C$ of soil CO_2 efflux was −25.0‰, and after 4.4 d it reached the steady-state value within 0.1‰. The decrease was faster when dissolution of CO_2 in soil water was disregarded: 1 h after the switch, $\delta^{13}C$ of the soil CO_2 efflux was −26.3‰, and after 6 h it differed less than 0.1‰ from the steady-state value. The timescale differed by a factor of 18, which was consistent with the ratio of total (gaseous + aquatic phase) CO_2 to gaseous CO_2 in the soil. When the system was in steady-state under labelling conditions, a step change in $\delta^{13}C$ back to the ambient value of −8.5‰ caused analogous changes in the other direction, including a shift in $\delta^{13}C$ of soil CO_2 efflux to 29.4‰ more depleted values (Fig. 3.3 b). This appeared as a tracer in the soil CO_2 efflux, while the isotopic signal of respiratory

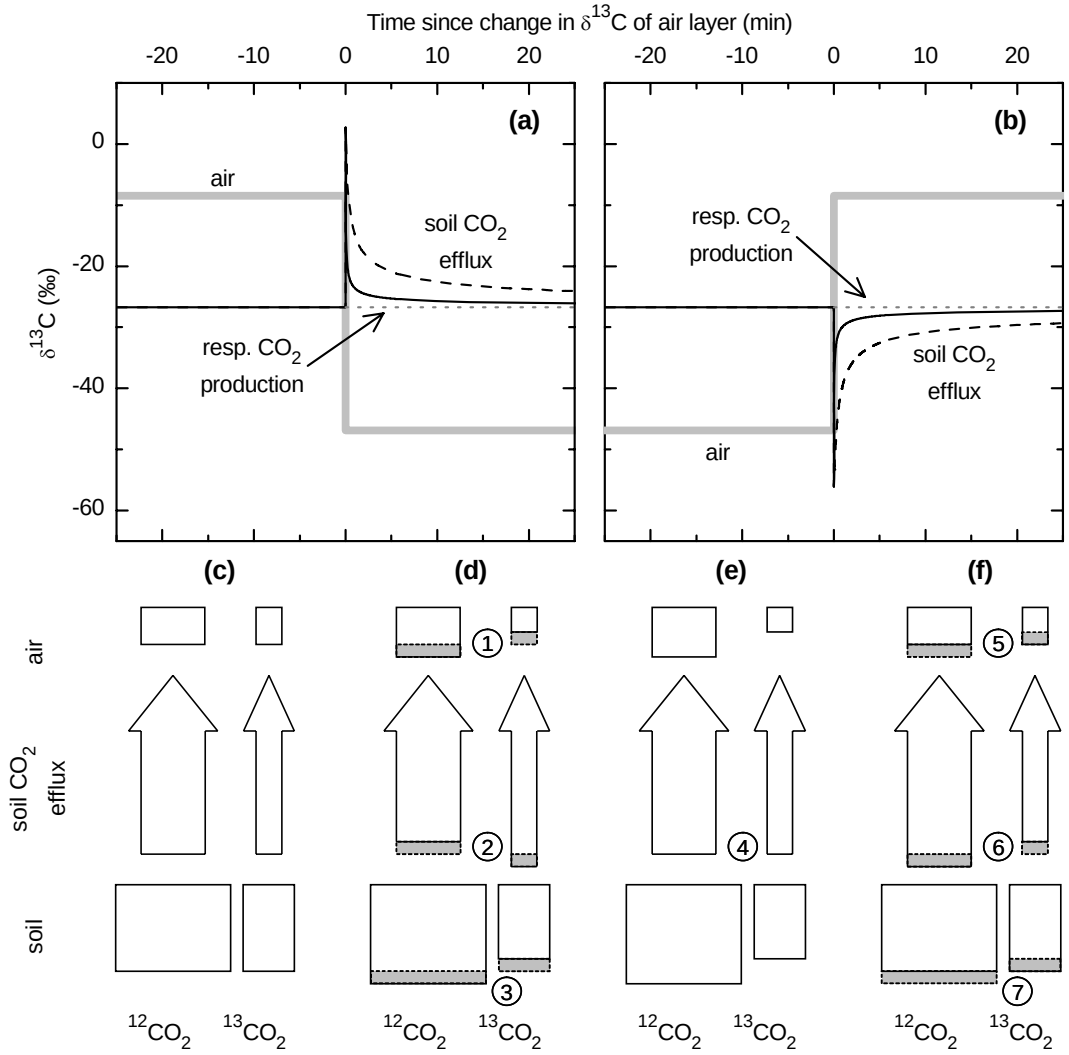

Figure 3.3: Influence of a step change in $\delta^{13}C$ in the air layer on $\delta^{13}C$ of soil CO_2 efflux. Top (a and b): $\delta^{13}C$ of soil CO_2 efflux when dissolution of CO_2 in soil water was regarded (black solid line) or disregarded (black dashed line). $\delta^{13}C$ in the air layer (thick grey line) was switched (a) from ambient (−8.5‰) to labelling conditions (−46.9‰), and (b) from labelling to ambient conditions. Before the switches, the soil-air system was in steady-state. $\delta^{13}C$ of respiratory CO_2 production (grey dotted line) in the soil was constant at −26.7‰. Bottom: Schematic illustration of the mechanism underlying abiotic tracer flux, considering $^{12}CO_2$ and $^{13}CO_2$ as separate diffusing gases. Squares, CO_2 pools in the air and in the soil; arrows, CO_2 fluxes. (c) Unlabelled system in steady-state. (d) Tracer application and associated transitions, namely (1) change in CO_2 in air layer to more depleted $\delta^{13}C$, (2) change in CO_2 diffusive fluxes due to changes in soil-air CO_2 gradient, and (3) change in soil CO_2 reservoir due to changed fluxes. (e) Labelled system in steady-state with (4) fluxes exhibiting the original isotopic composition. (f) Closed chamber measurement and associated transitions, namely (5) change in CO_2 in air layer to $\delta^{13}C$ of ambient air, (6) change in CO_2 diffusive fluxes due to changes in soil-air CO_2 gradient, and (7) change in soil CO_2 reservoir due to changed fluxes.

CO_2 was constant at $-26.7‰$ during the whole simulation run.

The following mechanism underlied these simulation results, which were derived from the parallel consideration of $^{12}CO_2$ and $^{13}CO_2$ (Fig. 3.3 c–f). (1) The change of $\delta^{13}C$ of CO_2 in the air layer from ambient to labelling (more depleted) conditions corresponded to an increase of the air $^{12}CO_2$ pool and a decrease of the air $^{13}CO_2$ pool. (2) These changes of CO_2 pool sizes in the air layer caused changes in the CO_2 gradients between soil and air, resulting in decreased $^{12}CO_2$ and increased $^{13}CO_2$ diffusive soil effluxes. (3) These changed fluxes, in turn, increased the soil pool of $^{12}CO_2$ and decreased that of $^{13}CO_2$. (4) After some time, the system attained a new equilibrium with the original fluxes, but with changed isotopic signatures of the air and soil CO_2 pools. In total, the atmospheric tracer signal was transmitted into the soil, even when both the $^{12}CO_2$ and the $^{13}CO_2$ flux were directed from the soil to the air layer. (5) The switch back to $\delta^{13}C$ of ambient air again changed the air CO_2 pool sizes, in this case $^{12}CO_2$ was decreased and $^{13}CO_2$ was increased. (6) This led to increased $^{12}CO_2$ and decreased $^{13}CO_2$ soil efflux, thus to a change in $\delta^{13}C$ of the efflux to a more depleted value. This apparent tracer flux is of physical origin, and is termed abiotic tracer flux (in contrast to biological label return by respiration of previously assimilated tracer). It should be noted that the $^{12}CO_2$ and $^{13}CO_2$ pool sizes and fluxes changed, while total CO_2, which is the sum of both isotopologues, remained constant.

Simulated tracer kinetics of ecosystem respiration

The simulation of the labelling experiment predicted $\delta^{13}C$ of soil CO_2 efflux, which was obtained from Keeling plot intercepts (Fig. 3.4, thin lines), to be depleted compared to ecosystem respiratory CO_2 production (Fig. 3.4, thick line). The average predicted bias due to the change in chamber headspace air at closure was $1.0‰$ in the labelled ecosystem (Fig. 3.4 a, thin black solid line). This corresponded to a step change in $\delta^{13}C$ in the air layer from labelling to ambient conditions (see Fig. 3.1 and Fig. 3.3 b,e,f). Besides the abiotic tracer signal considered in the above illustration of changes in the air layer $\delta^{13}C$, also biological tracer flux (due to increasing respiration of label) occurred in the course of the labelling experiment. Additional consideration of dissolution of CO_2 in soil water (Fig. 3.4 b, thin black solid line) or downwards displacement of soil air (Fig. 3.4 a, thin blue dashed line) increased the predicted bias to $4.2‰$ and $3.6‰$, respectively. The bias reached $9.2‰$, when all three mechansims (change in headspace air, dissolution

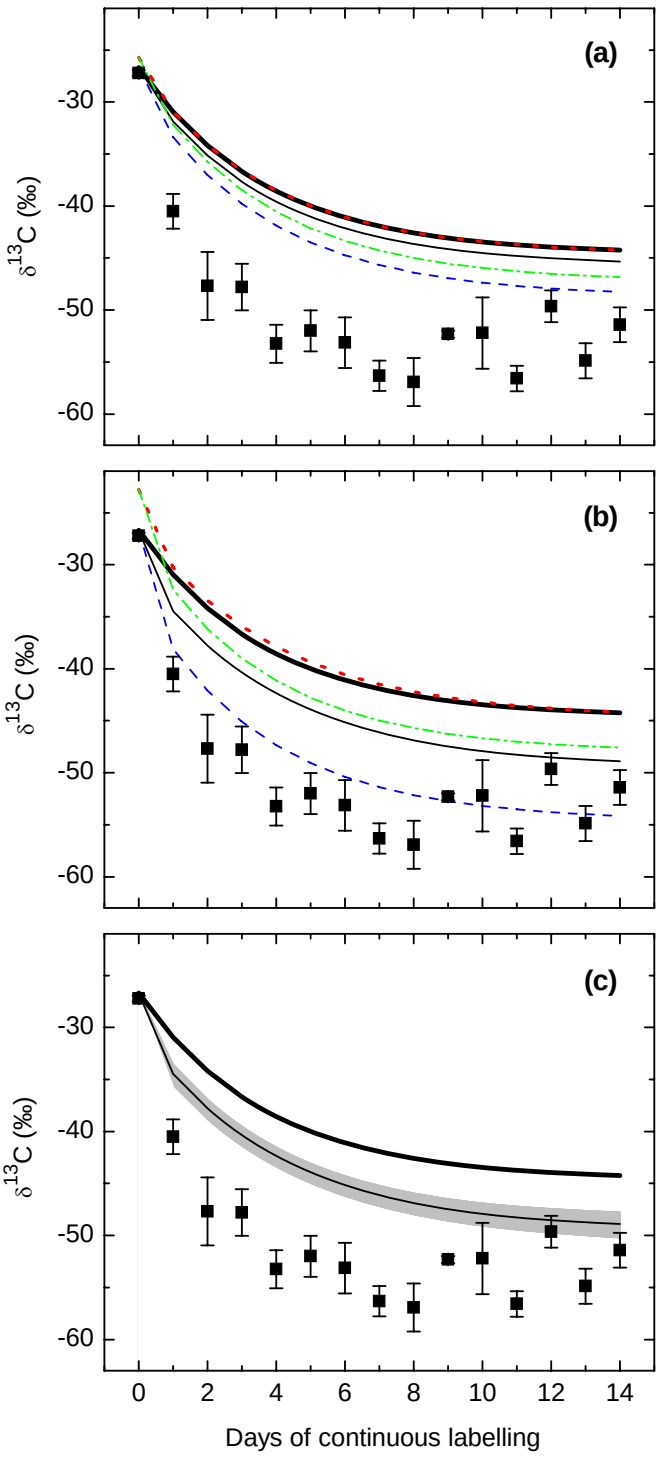

Figure 3.4: $\delta^{13}C$ of ecosystem respiratory CO_2 production (thick black line), measured by the open chamber approach, and $\delta^{13}C$ of soil CO_2 efflux, derived from measured (filled squares; error bars: standard error, $n = 2$–10) and simulated (thin lines) Keeling plot intercepts in closed chambers. Simulations (a) disregarded and (b) considered dissolution of CO_2 in soil water, with CO_2 at chamber closure changed to ambient conditions (see Fig. 3.1) and downwards displacement of soil air disregarded (black solid) and considered (blue dashed). Red and green lines in (a) and (b) indicate simulations where CO_2 at chamber closure was not changed to ambient conditions but remained constant at labelling conditions; again when soil air displacement was disregarded (red dotted) and considered (green dashed-dotted). (c) The grey shaded area indicates the sensitivity of model predicted Keeling plot intercepts to variations of input parameters (see Table 3.1 for range). This sensitivity analysis was performed for the simulation run considering dissolution and disregarding displacement (thin solid line).

and displacement) were considered simultanously (Fig. 3.4 b, thin blue dashed line). The magnitude of the bias caused by Keeling plot non-linearity was derived from simulations where δ^{13}C of chamber headspace air remained unchanged and displacement of soil air did not occur. These conditions were approximately met during Keeling plot sampling in the non-labelled ecosytem (0 days of continuous labelling; see also Fig. 3.1), where the bias was no larger than 0.1‰. Similarily, simulated Keeling plot intercepts ranged within 0.1‰ compared to respiratory CO_2 production at the end of the labelling experiment, when δ^{13}C in the air layer was held constant under labelling conditions (Fig. 3.4 a,b, thin red dotted lines). In this case, the bias caused by displacement of soil air was within 2.9‰ (Fig. 3.4 a,b, thin green dashed-dotted lines). Sensitivity of the simulated Keeling plot intercepts to uncertainties in the model input parameters, namely soil respiration rate, depth distribution of CO_2 production in soil, soil porosity, temperature and pH, was within 1.5‰ (Fig. 3.4 c).

Experimental tracer kinetics of ecosystem respiration

The observed bias between Keeling plot intercepts measured in closed chambers (Fig. 3.4, filled squares) and respiratory CO_2 production (Fig. 3.4, thick line) was on average 11.2‰ in the labelled ecosystem. In contrast, the control measurements (before labelling started) did not differ significantly ($P = 0.31$). Comparison of the observed Keeling plot intercepts with the model predictions showed that the simulation including all three mechansims (change in headspace air, dissolution and displacement) essentially explained the observed bias. On the other hand, simulations including a change in headspace air and either dissolution or displacement or none of these effects accounted for less than half of the observed bias. The sensitivity of model predictions to uncertainties in the input parameters was relatively small. It did not allow to explain the observed bias without taking dissolution and displacement into account (Fig. 3.4 c). This strongly suggests that, besides diffusion, both dissolution and displacement played a significant role in closed chamber Keeling plots in the continuous labelling experiment. Processes which were not comprised in the simulation accounted for the remaining deviation of 2.0‰ between modelled and observed tracer kinetics. These processes included temporal changes of parameters during the course of the labelling experiment, diffusion in the aquatic phase, displacement of soil water or incomplete isotopic equilibration between gaseous and dissolved CO_2.

Discussion

Mechanisms which influenced δ^{13}C of nighttime soil CO_2 efflux

In the continuous labelling experiment, three mechanisms contributed significantly to the difference between the isotopic composition of soil CO_2 efflux observed with closed chambers and respiratory CO_2 production: (1) the change in isotopic composition of CO_2 in chamber air, (2) the dissolution of label CO_2 in soil water, and (3) the displacement of soil air. This corresponded with the idea that labelling CO_2 penetrated into soil pores during tracer application and emerged — driven by altered $^{12}CO_2$ and $^{13}CO_2$ concentration gradients — into chamber air during subsequent closed chamber respiration measurements. More precisely, the observed decrease of 11.2‰ in δ^{13}C of ecosystem respired CO_2 corresponded to a 29% increase in the fraction of labelled CO_2. Compared to this, the impact of artefacts specific to Keeling plots was negligible.

The change in isotopic composition of chamber air at the beginning of the closed chamber measurement was a prerequisite for abiotic tracer efflux. The size of this effect of approx. 1‰ corresponded to the magnitude estimated by Nickerson & Risk (2009c) for a sharp concentration decrease of headspace CO_2, which caused similar perturbation as switching from daytime labelling to closed chamber respiration measurements. They reported a range of 0–15‰. Compared to the parameter range used in that study, site conditions of the present study were such that the simulated bias was expected to range in the lower part of 0–15‰ given by Nickerson & Risk.

Dissolution of CO_2 in soil water provided a large reservoir in the soil, which allowed storage of additional label CO_2. Dissolution of CO_2 delayed equilibration between soil CO_2 and overlying atmosphere, and thus changes in δ^{13}C of soil CO_2 efflux lagged. As a result, the theoretical bias increased from 1.0‰ to 4.2‰. To allow dissolved CO_2 to participate in CO_2 gas transport, instantaneous exchange between gaseous and dissolved phase was assumed. This requirement was sufficiently fulfilled when the gaseous-dissolved phase equilibration was fast compared to the isotopic equilibration between soil air CO_2 and overlying atmosphere, which occured within hours to days. Presumably, this was the case as carbonic anhydrase, which catalyses the gaseous-dissolved phase equilibration of CO_2, was previously found in soil-inhabitating organisms such as bacteria (Kusian *et al.*, 2002; Mitsuhashi *et al.*, 2004) and fungi (Aguilera *et al.*, 2005; Amoroso *et al.*, 2005; Klengel

et al., 2005; Mogensen *et al.*, 2006), as well as in non-photosynthetic plant organs and tissues (Raven & Newman, 1994), particularly roots (Viktor & Cramer, 2005) and growing root tips (Chang & Roberts, 1992). Furthermore, Seibt *et al.* (2006) and Wingate *et al.* (2008) provided evidence for the presence of carbonic anhydrase in the upper soil, which accelerates the hydration of bicarbonate by a factor of 80–1000 (which corresponded to equilibration within less than 1 s). Considering these timescales, participation of a major fraction of dissolved CO_2 in soil gas transport is likely, even if isotopic equilibrium was not fully reached. Such incomplete equilibration was reported by Gillon & Yakir (2001) for oxygen isotopes in leaves. These findings corresponded with the suggestion of Högberg *et al.* (2008), that during tracer application CO_2 in soil air and in carbonic acid in soil water had, at least partly, equilibrated isotopically with the labelling CO_2.

Downwards displacement of soil air biased nighttime respiration measurements, even when the displacement occured before the measurements. As overpressure occurred inside the chamber headspace during daytime tracer application (Gamnitzer *et al.*, 2009), we suppose that soil air masses were displaced downwards, according to the mechanism described by Lund *et al.* (1999) and considering suppression of lateral movement by soil collars. Furthermore, CO_2 concentration measured in soil air beneath the chambers (U. Gamnitzer, unpublished data) decreased during tracer application, which is consistent with the downwards displacement of soil air. The air mass flow caused labelling CO_2 to penetrate deeper into the soil, resulting in increased isotopic disequilibrium fluxes and thus up to 5.0‰ more depleted soil CO_2 efflux.

The soil air model captured the dominant mechanisms which determined the observed bias. Compared to these processes, known artefacts specific to Keeling plots were of little importance. So deviations due to inappropriate application of regression models (ordinary least square regression versus geometric mean regression; see Pataki *et al.* 2003; Zobitz *et al.* 2006) were 0.09‰ on average. Also CO_2 accumulating in the closed chamber headspace and associated chamber-soil feedbacks (Nickerson & Risk, 2009b) caused only little variation of the Keeling plot intercepts under the prevailing site conditions, which included short chamber deployment times as well as relatively low diffusivity and high respiration rate. For ecosystems where soil CO_2 was in equilibrium with the overlying atmosphere at chamber closure, simulated Keeling plot intercepts agreed within 0.1‰ with $\delta^{13}C$ of respiratory CO_2 production, compared to a difference of up to 4‰ estimated by Nickerson & Risk (2009b) for a variety of soil conditions.

Implications for respiration measurements

The exemplary study of soil CO_2 transport in a labelled ecosystem revealed two mechanisms which are potentially relevant in various investigations of soil and ecosystem respiration: (1) abiotic variations in $\delta^{13}C$ of soil CO_2 efflux distorted the observation of belowground respiratory CO_2 production, and (2) enlargement of the soil CO_2 pool by exchange of CO_2 between air and water pores extended transient changes in $\delta^{13}C$ of soil CO_2 efflux. The present study surveyed non-steady-state effects on ecosystem respiration measurements. Compared to that, the distortion of soil respiration measurements is supposed to be even larger. Ecosystem respiration includes belowground (soil) respiration as well as aboveground respiration, where the latter does not affect soil CO_2 storage. Thus, the bias of the belowground respiratory signal is attenuated by mixing with the unbiased aboveground signal.

Measurements of $\delta^{13}C$ of belowground respiratory CO_2 production by observation of soil CO_2 efflux are sensitive to changes in $\delta^{13}C$ in the air above the soil, as demonstrated in the case of closed chamber Keeling plots in a labelled ecosystem. This agreed with observations of Ohlsson *et al.* (2005), that Keeling plot intercepts depended on chamber air treatment prior to the measurement. Furthermore, the experimental evidence of non-steady-state effects was consistent with a theoretical investigation of commonly applied techniques altering the soil-atmosphere gradient (Nickerson & Risk, 2009c). Among them were non-steady-state chambers where the CO_2 concentration was lowered at closure (Flanagan *et al.*, 1996; Buchmann & Ehleringer, 1998; Ohlsson *et al.*, 2005) and flow-through chambers supplied with CO_2-free air (Andrews & Schlesinger, 2001; Bernhardt *et al.*, 2006; Midwood *et al.*, 2008).

Large changes in $\delta^{13}C$ of CO_2 in the air layer and thus in soil CO_2 efflux are induced by isotope tracer application via photosynthetic uptake of labelled CO_2. Subke *et al.* (2009) detected abiotic tracer fluxes when labelling CO_2 contained 21% of $^{13}CO_2$ (corresponding to $\delta^{13}C$ of 23000‰). The current study corroborates this finding for a much smaller labelling signal of ∼40‰. This also indicates, that abiotic tracer fluxes can occur in FACE experiments, which are usually operated at $\delta^{13}C$ of elevated CO_2 between −15‰ and −20‰ (e.g. Nitschelm *et al.*, 1997; Matamala *et al.*, 2003; Asshoff *et al.*, 2006; Keel *et al.*, 2006; Pregitzer *et al.*, 2006; Taneva *et al.*, 2006). When FACE experiments are combined with measurements of soil respiratory $\delta^{13}C$ (Torn *et al.*, 2003; Søe *et al.*, 2004; Pregitzer *et al.*, 2006; Taneva *et al.*, 2006) and fumigation with isotopically different CO_2

is restricted to daytime (e.g. Lewin *et al.*, 1994; Zanetti *et al.*, 1996; Miglietta *et al.*, 1997; Hendrey *et al.*, 1999; Dickson *et al.*, 2000; Edwards *et al.*, 2001; Miglietta *et al.*, 2001; Reich *et al.*, 2001; Pepin & Körner, 2002), the measurements are potentially biased when performed subsequent to day-night tracer switches. Soil-air disequilibria are also imposed prior to respiration measurements in pulse labelling experiments. However, the timescale on which abiotic tracer fluxes are large enough to be detected must be considered. It ranged from hours to days in our example, which is consistent with observations in a forest ecosystem, where the abiotic tracer flux was significant for 48 h (Subke *et al.*, 2009).

Enlargement of the soil CO_2 pool has the potential to amplify known non-steady-state effects induced by chamber measurement procedures, natural variability and also tracer application. Thus, the bias due to chamber-induced disequilibria might exceed the 15‰ predicted by Nickerson & Risk (2009c) for consideration of CO_2 in soil air. Natural variability in atmospheric CO_2 causes the same effect on soil CO_2 efflux as a change of headspace CO_2 inside the chambers, but with smaller magnitude. Nickerson & Risk (2009a) predicted a bias of up to 0.05‰ due to daytime-nighttime changes of both atmospheric CO_2 concentration and isotopic composition, with the individual effects nearly cancelling each other out. When this is multiplied by a factor of 18 due to enlarged soil CO_2 pool, the bias is 1‰, which is detectable with respect to the precision of common mass spectrometric technique (see e.g. Schnyder *et al.*, 2004). As the amount of CO_2 in the dissolved phase increases with pH and with soil water content, the effect of enlarged soil CO_2 pool on soil CO_2 efflux is expected to be largest under alkaline and wet conditions.

In conclusion, the soil CO_2 transport model predicted the impact of non-steady-states on measurements of isotopic composition of soil CO_2 efflux, as it captured the dominant mechanisms. Thus, it enabled estimation of potential biases in isotopic measurements of soil and ecosystem respiration. It demonstrated that CO_2 isotopic composition in air needs to be carefully chosen to keep steady-state in terms of isotopic composition of soil CO_2 efflux, in particular in labelled environments. This has been shown for the example of closed chamber Keeling plot measurements, but it applies also in other measurement circumstances. For example in open flow-through chambers headspace air CO_2 needs to be maintained at predefined conditions. Dissolution of CO_2 in soil water turned out to amplify non-steady-state effects by influencing the magnitude of transient processes, while it had no influence on depth profiles in the steady-state.

4 Summarising discussion

Methodological advances

In this study, a new tracer technique was established to investigate C allocation and partitioning in a grassland ecosystem by continuous $^{13}CO_2/^{12}CO_2$ labelling, similar to the techniques successfully applied in laboratory experiments (Deléens *et al.*, 1983; Schnyder, 1992; Schnyder *et al.*, 2003). The new open-top chamber apparatus provided both precise application of the tracer under near-natural environmental conditions and accurate analysis of the tracer content in ecosystem respired CO_2 online in the field. The challenge of maintaining constant isotopic composition during daytime tracer application was overcome by high air flow through the chamber and by minimised ambient air incursion through the buffered vent (Fig. 2.4). Despite the feedback of the enclosed ecosystem on chamber headspace CO_2, the $\delta^{13}C$ of the labelling CO_2 was stable within 0.4‰ (SD including day-to-day variation) during the entire labelling period (Fig. 2.7 b). For comparison, $\delta^{13}C$ was constant within 0.2–0.3‰ in stand-scale experiments in growth chambers (Schnyder *et al.*, 2003; Lehmeier *et al.*, 2010). On the other hand, the difference between the isotopic composition of the tracer (−46.9‰) and natural CO_2 (−8.5‰) was approx. 100 times larger than the achieved precision. Apart from the alteration in the isotopic composition of CO_2, environmental conditions inside the open-top chambers ranged well within conditions occuring naturally at the field site (Figs. 2.6 and 2.7 a). Besides the investigation of C supply to ecosystem respiration, the tracer technique presented here also enables the study of C allocation to plant growth (I. Schleip, unpublished data) and to the soil compartment (E. Kaštovská, unpublished data) under field conditions.

Comprehensive investigation of the two different measurement modes applied for tracer analysis in nighttime ecosystem respiration revealed the following: (1) The tracer content of ecosystem respired CO_2 was measured accurately and precisely in the open chamber mode. That open-chamber measurements were accurate was supported by reference

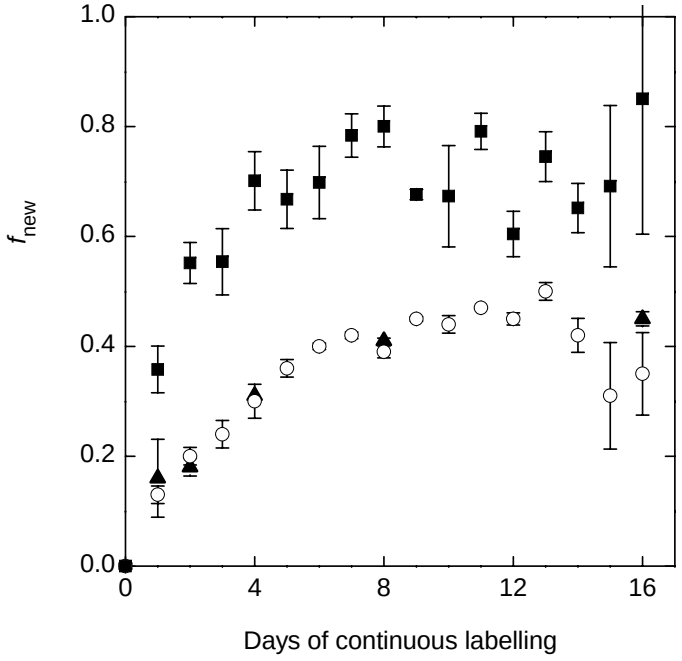

Figure 4.1: Tracer kinetics of ecosystem respired CO_2 (fraction of labelled C, f_{new}), obtained with different measurement methods during a 16 days-long continuous labelling experiment. Open circles, steady-state open chamber measurements online in the field (Fig. 2.8); closed triangles, laboratory-based reference measurements on excised soil+vegetation blocks under controlled conditions (Fig. 2.8); closed squares, Keeling plot intercepts derived from non-steady-state closed chamber measurements (Fig. 3.4). Error bars indicate SE ($n = 2$–10).

measurements (Fig. 2.8, see also Fig. 4.1) with an independent, established, laboratory-based method (Lötscher *et al.*, 2004). The operation at nearly constant $\delta^{13}C$ of chamber headspace CO_2 was essential for preventing imbalances between CO_2 respired belowground and soil CO_2 efflux (Fig. 3.3). (2) Measurements obtained with the closed chamber approach were clearly biased. They suggested approx. 1.5-fold tracer content compared to the open chamber and reference measurements (Fig. 4.1). This bias could be largely explained by penetration of tracer into soil pores during daytime tracer application and subsequent release into chamber air during nighttime measurements. Non-biological tracer return has been previously noted in applications using highly enriched $^{13}CO_2$ (Staddon *et al.*, 2003; Leake *et al.*, 2006; Subke *et al.*, 2009). The present work provides a mechanistic model of these effects and demonstrates for the first time, that non-biological tracer return occurred in labelling studies using near-natural abundance of $^{13}CO_2/^{12}CO_2$. Thus, operating conditions of respiration chambers need to be carefully selected, particularly in free-air CO_2 enrichment (FACE) experiments.

Kinetic characteristics of C turnover in a grassland ecosystem

Compartmental analysis (Atkins, 1969; Jacquez, 1996) of the observed tracer kinetics revealed that ecosystem respiration at ambient CO_2 concentration was supplied by two

kinetically distinct sources. One was closely connected with current photosynthetic activity and largely corresponded with autotrophic respiration (i.e. shoot, root and rhizosphere respiration). The other source was supplied by substrate pools that released C only after long residence time ($\geq$ months) in the ecosystem. This source was thus considered to represent the heterotrophic component of ecosystem respiration (i.e. decomposition of old organic material).

Prerequisites for compartmental analysis

Application of the two-pool compartmental model required that the kinetic characteristics of the two sources did not change during the whole labelling experiment, i.e. the system had to be in a steady-state apart from the increase in tracer content. In particular, the relative contributions from the two sources and the mean residence time of C in the rapidly turned over pool were assumed to be constant on a day-to-day basis. Certainly, these conditions were not exactly met in the field experiment. The allocation of assimilate within the plant is generally thought to be determined by source-sink interactions, which in turn may vary with environmental conditions (see e.g. Dickson, 1991; Stitt & Schulze, 1994). In a pulse labelling experiment, the observed tracer allocation pattern strongly depends on the actual conditions during the short period of tracer uptake. So, rapid fluctuations in climatic conditions may complicate the interpretation of tracer kinetics in such studies. In contrast, the continuous labelling approach used in the present study integrated over variations during the entire study period, providing insight into the average C allocation pattern. That the present study assessed the average C allocation pattern was also supported by the sampling scheme, which provided a larger number of replicate respiration measurements shortly after the onset of labelling. This ensured more reliable capture of average environmental conditions during the period of the steepest increase in tracer content. Moreover, green shoot biomass as well as root biomass did not change significantly during the experiment ($P = 0.20$ and $P = 0.30$, respectively; I. Schleip, unpublished data), indicating negligible plant growth. This further supported the steady-state assumption.

C residence times obtained in the field and in controlled environments

The observed mean residence time (3.7 d) of C in the rapidly labelled component of the respiratory substrate supply system was well within the range expected from controlled

environment studies on *Lolium perenne*. This species was a main component of the grassland under study. On the stand-scale, the tracer kinetics reported by Schnyder *et al.* (2003) reflected a mean residence time of 2.2 d. In plants grown under continuous light and ample nitrogen supply, Lehmeier *et al.* (2010) found a mean residence time of 4.6 d. This doubled under nitrogen deficient conditions. On the other hand, exposing the plants grown at high nitrogen to day/night cycles approximately halved the mean residence time (C. Lehmeier, unpublished data). Considering that the latter plants exhibited larger nitrogen content than the plants at the field site (I. Schleip, unpublished data), the mean residence time of C observed in the present field study was well within the range of that in controlled conditions.

Further differentiation of recently assimilated substrate

Further differentiation of the source supplying recent assimilates to respiration was not possible due to the time resolution of labelling of 1 d (more precisely, one whole light period). A major part of respiration from this source was constituted by plant shoot and root respiration. Indeed, there is increasing evidence that plant respiration is supplied by kinetically distinct substrate pools (including organic compounds from current photosynthesis as well as temporarily stored substrate) with half-lives from less than 1 h to more than 1 week (Ryle *et al.*, 1976; Schnyder *et al.*, 2003; Lehmeier *et al.*, 2008, 2010). These studies suggest, that the source supplying recent assimilates to ecosystem respiration comprised several 'subpools', whose size, turnover and interactions determined the residence time of C. However accurate determination of the mean residence time required equal consideration of both the rapidly and the slowly turned over subpools. In the present study this was provided by the continuous application of the tracer.

To increase time resolution in future studies, the onset of labelling could be shifted from sunrise to various times during the day. Then the first nighttime respiration measurement would occur after less than a whole light period of labelling. Also darkening of the chambers during daytime provides an opportunity to measure respiration after less than a whole day of labelling. However, diurnal variations in C allocation have been noted in day-night cycles due to filling and depletion of storage pools (Farrar & Farrar, 1986; Gibon *et al.*, 2004), which needs to be accounted for in compartmental analysis of such a tracer kinetics. For this purpose, the high time resolution of the online respiration measurement technique ($\sim$15 min) could be helpful. However, isotopic imbalances between respiratory CO_2 pro-

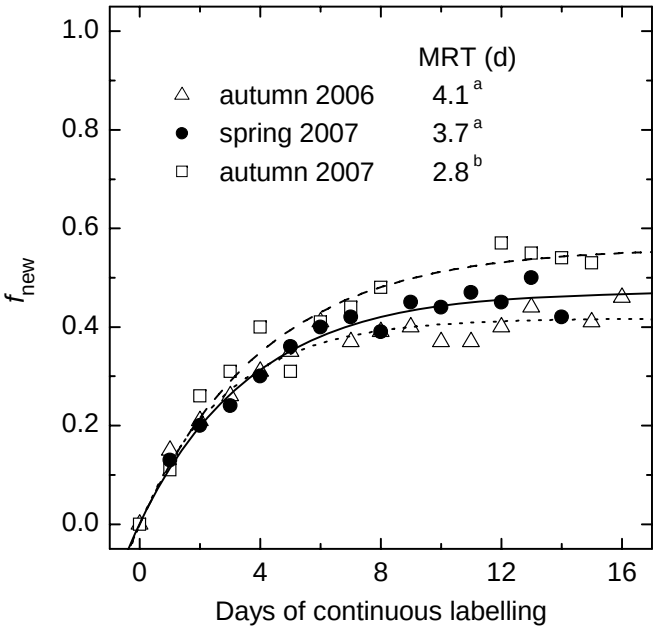

Figure 4.2: Tracer kinetics of ecosystem respired CO_2 (fraction of labelled C, f_{new}), observed during 2-weeks long continuous labelling experiments in autumn 2006 (28 Aug. – 13 Sept.; open squares), spring 2007 (13 May – 29 May; closed circles) and autumn 2007 (10 Sept. – 26 Sept.; open triangles) at Grünschwaige Grassland Research Station. Respiration measurements were obtained with a steady-state open chamber technique at night (see Chapter 2). For each of the tracer kinetics, the two-source model described by $f_{new}(t) = a(1 - e^{-bt})$ (Eqn. 2.6) was the simplest model that captured the key characteristics (dashed line, autumn 2006; solid line, spring 2007; dotted line, autumn 2007). More complex models were not supported by the data. Thus the same model structure reflected the substrate supply system for ecosystem respiration in the three investigated periods. The mean residence time (MRT) of C in the substrate pool of autotrophic respiration was given by the fit parameter b, $MRT = 1/b$. Shared superscripts indicate that values did not differ significantly ($P < 0.05$).

duction and soil CO_2 efflux are expected to become increasingly important with higher time resolution (see Fig. 3.3 as an example). The soil CO_2 transport model established in Chapter 3 might be a useful tool to further investigate this.

Seasonal and interannual variation of respiratory substrate supply

With the new tracer technology presented in this work, seasonal and interannual variations in the substrate supply to ecosystem respiration can now be explored. This is supported by comparison of tracer kinetics obtained at the same site but in different seasons and years (Fig. 4.2). These tracer kinetics had similar shape and thus obeyed the two-pool model

introduced in Chapter 2. But they differed in relative contributions from the two sources supplying ecosystem respiration and in the mean residence time of C in the rapidly turned over source. Enhanced growth, which usually occurs in spring, may result in shorter mean residence time of C in this source: at the plant level, growth respiration was identified to be closely connected to C assimilated within the preceding light period, while 'older' (i.e. stored) C was primarily related to maintainance respiration (Lötscher *et al.*, 2004). Considering the subpools which constitute the source identified as 'recently assimilated C' in the present study, this suggests reduced mean residence time in the case of enhanced growth. However, a clear seasonal pattern with shorter residence time in spring was not evident in the present study, in contrast to the observations of Carbone & Trumbore (2007). Perhaps the seasonal pattern was masked by interannual variability. Such variability might be connected with differences in the size of the pool supplying recently assimilated C to ecosystem respiration. Shoot biomass was identified to comprise the main fraction of the total substrate pool supplying shoot and root respiration (Lehmeier *et al.*, 2008). Between the three labelling experiments discussed here, shoot biomass varied by a factor of 2–3 (I. Schleip, unpublished data). This suggested that the turnover was largely determined by the size of the canopy. To quantitatively understand the mechanisms behind, further investigations are necessary. These could include the involvement of non-structural carbohydrates in plant biomass, because these are generally considered as the main source of respired C within plants (ap Rees, 1980; Tcherkez *et al.*, 2003).

Outlook: further potential applications

In conclusion, the new labelling technology introduced in the present work was established as a unique tool to partition the C sources of ecosystem respiration into recent assimilates and old organic matter, and to quantify the turnover of the autotrophic pool. How the kinetic characteristics, which were determined for the grassland under study, transfer to other ecosystems, needs further investigation. For example, distinct patterns of C allocation were reported for grassland and shrub ecosystems (Carbone & Trumbore, 2007). The open-top chamber system introduced here is well suited for investigations of grasslands or other types of vegetation with low canopy height. In comparison, trees would require much larger chambers. However, in practice, the chamber size is likely to be limited by the technical feasibility to supply a sufficient amount of CO_2-free air. The new system provides the opportunity for field labelling studies at any CO_2 concentration, from subambient to

elevated CO_2, and investigation of a large range of factors potentially influencing ecosystem C allocation and turnover. Among these are nitrogen supply (Lehmeier *et al.*, 2010), defoliation (Lattanzi *et al.*, 2004; Lehmeier, 2008), arbuscular mycorrhizal colonisation (Grimoldi *et al.*, 2006), liming (Staddon *et al.*, 2003) or shading (Bahn *et al.*, 2009), which are all of great ecological significance.

Bibliography

Aguilera J, Van Dijken JP, De Winde JH, Pronk JT (2005) Carbonic anhydrase (NCE103p): An essential biosynthetic enzyme for growth of *Saccharomyces cerevisiae* at atmospheric carbon dioxide pressure. *Biochemical Journal* **391**: 311–316.

Amoroso G, Morell-Avrahov L, Müller D, Klug K, Sültemeyer D (2005) The gene NCE103 (YNL036w) from *Saccharomyces cerevisiae* encodes a functional carbonic anhydrase and its transcription is regulated by the concentration of inorganic carbon in the medium. *Molecular Microbiology* **56**: 549–558.

Amundson R, Stern L, Baisden T, Wang Y (1998) The isotopic composition of soil and soil-respired CO_2. *Geoderma* **82**: 83–114.

Andrews JA, Schlesinger WH (2001) Soil CO_2 dynamics, acidification, and chemical weathering in a temperate forest with experimental CO_2 enrichment. *Global Biogeochemical Cycles* **15**: 149–162.

Andrews JA, Harrison KG, Matamala R, Schlesinger WH (1999) Separation of root respiration from total soil respiration using ^{13}C labeling during free-air carbon dioxide enrichment (FACE). *Soil Science Society of America Journal* **63**: 1429–1435.

ap Rees T (1980) Assessment of the contributions of metabolic pathways to plant respiration. *In* DD Davies, ed, *The Biochemistry of Plants: A Comprehensive Treatise, Vol. 2.* Academic Press, San Diego, CA, USA, pp 1–29.

Asshoff R, Zotz G, Körner C (2006) Growth and phenology of mature temperate forest trees in elevated CO_2. *Global Change Biology* **12**: 848–861.

Atkins GL (1969) *Multicompartment Models in Biological Systems.* Methuen & Co. Ltd., London, UK.

Bahn M, Schmitt M, Siegwolf R, Richter A, Brüggemann N (2009) Does photosynthesis affect grassland soil-respired CO_2 and its carbon isotope composition on a diurnal timescale? *New Phytologist* **182**: 451–460.

Baldocchi DD, White R, Johnston JW (1989) A wind-tunnel study to design large, open-top chambers for whole-tree pollutant exposure experiments. *Japca – The Journal of the Air & Waste Management Association* **39**: 1549–1556.

Bernhardt ES, Barber JJ, Pippen JS, Taneva L, Andrews JA, Schlesinger WH (2006) Long-term effects of free air CO_2 enrichment (FACE) on soil respiration. *Biogeochemistry* **77**: 91–116.

Buchmann N, Ehleringer JR (1998) CO_2 concentration profiles, and carbon and oxygen isotopes in C3, and C4 crop canopies. *Agricultural and Forest Meteorology* **89**: 45–58.

Campbell GS, Norman JM (1998) *An Introduction to Environmental Biophysics.* Springer, New York, NY, USA.

Carbone MS, Trumbore SE (2007) Contribution of new photosynthetic assimilates to respiration by perennial grasses and shrubs: residence times and allocation patterns. *New Phytologist* **176**: 124–135.

Carbone MS, Czimczik CI, McDuffee KE, Trumbore SE (2007) Allocation and residence time of photosynthetic products in a boreal forest using a low-level ^{14}C pulse-chase labeling technique. *Global Change Biology* **13**: 466–477.

Cerling TE (1984) The stable isotopic composition of modern soil carbonate and its relationship to climate. *Earth and Planetary Science Letters* **71**: 229–240.

Chang KJ, Roberts JKM (1992) Quantitation of rates of transport, metabolic fluxes, and cytoplasmic levels of inorganic carbon in maize root-tips during K^+ ion uptake. *Plant Physiology* **99**: 291–297.

Chapin FS, Woodwell GM, Randerson JT, Rastetter EB, Lovett GM, Baldocchi DD, Clark DA, Harmon ME, Schimel DS, Valentini R *et al.* (2006) Reconciling carbon-cycle concepts, terminology, and methods. *Ecosystems* **9**: 1041–1050.

Cisneros-Dozal LM, Trumbore S, Hanson PJ (2006) Partitioning sources of soil-respired CO_2 and their seasonal variation using a unique radiocarbon tracer. *Global Change Biology* **12**: 194–204.

Dawson TE, Mambelli S, Plamboeck AH, Templer PH, Tu KP (2002) Stable isotopes in plant ecology. *Annual Review of Ecology and Systematics* **33**: 507–559.

de Visser R, Vianden H, Schnyder H (1997) Kinetics and relative significance of remobilized and current C and N incorporation in leaf and root growth zones of *Lolium perenne* after defoliation: assessment by ^{13}C and ^{15}N steady-state labelling. *Plant Cell and Environment* **20**: 37–46.

Deléens E, Pavlides D, Queiroz O (1983) Natural ^{13}C abundance as a tracer for the determination of leaf matter turn-over in C3 plants. *Physiologie Vegetale* **21**: 723–729.

Dickson RE (1991) Assimilation distribution and storage. *In* AS Raghavendra, ed, *Physiology of Trees.* Wiley, New York, NY, USA, pp 51–85.

Dickson RE, Lewin KF, Isebrands JG, Coleman MD, Heilmann WE, Riemenschneider DE, Sober J, Host GE, Hendrey GR, Pregitzer KS *et al.* (2000) Forest atmosphere carbon transfer storage (FACTS-II) — the aspen free-air CO_2 and O_3 enrichment (FACE) project: an overview. Technical Report NC-214, USDA Forest Service, North Central Experiment Station. St. Paul, MN, USA.

Diemer M, Körner C, Prock S (1992) Leaf life spans in wild perennial herbaceous plants — a survey and attempts at a functional interpretation. *Oecologia* **89**: 10–16.

Dore S, Hymus GJ, Johnson DP, Hinkle CR, Valentini R, Drake BG (2003) Cross validation of open-top chamber and eddy covariance measurements of ecosystem CO_2 exchange in a Florida scrub-oak ecosystem. *Global Change Biology* **9**: 84–95.

Edwards GR, Clark H, Newton PCD (2001) The effects of elevated CO_2 on seed production and seedling recruitment in a sheep-grazed pasture. *Oecologia* **127**: 383–394.

Fang C, Moncrieff JB (1998) An open-top chamber for measuring soil respiration and the influence of pressure difference on CO_2 efflux measurement. *Functional Ecology* **12**: 319–325.

Farquhar GD, Lloyd J (1993) Carbon and oxygen isotope effects in the exchange of carbon dioxide between terrestrial plants and the atmosphere. *In* JR Ehleringer, AE Hall, GD Farquhar, eds, *Stable Isotopes and Plant Carbon-Water Relations.* Academic Press, New York, NY, USA, pp 47–70.

Farrar SC, Farrar JF (1986) Compartmentation and fluxes of sucrose in intact leaf blades of barley. *New Phytologist* **103**: 645–657.

Flanagan LB, Brooks JR, Varney GT, Berry SC, Ehleringer JR (1996) Carbon isotope discrimination during photosynthesis and the isotope ratio of respired CO_2 in boreal forest ecosystems. *Global Biogeochemical Cycles* **10**: 629–640.

Gamnitzer U, Schäufele R, Schnyder H (2009) Observing ^{13}C labelling kinetics in CO_2 respired by a temperate grassland ecosystem. *New Phytologist* **184**: 376–386.

Geiger DR (1980) Measurement of translocation. *Methods in Enzymology* **69**: 561–571.

Gibon Y, Bläsing OE, Palacios-Rojas N, Pankovic D, Hendriks JHM, Fisahn J, Höhne M, Günther M, Stitt M (2004) Adjustment of diurnal starch turnover to short days: depletion of sugar during the night leads to a temporary inhibition of carbohydrate utilization, accumulation of sugars and post-translational activation of ADP-glucose pyrophosphorylase in the following light period. *Plant Journal* **40**: 332.

Gillon J, Yakir D (2001) Influence of carbonic anhydrase activity in terrestrial vegetation on the ^{18}O content of atmospheric CO_2. *Science* **291**: 2584–2587.

Griffiths H (1991) Applications of stable isotope technology in physiological ecology. *Functional Ecology* **5**: 254–269.

Grimoldi AA, Kavanová M, Lattanzi FA, Schäufele R, Schnyder H (2006) Arbuscular mycorrhizal colonization on carbon economy in perennial ryegrass: quantification by $^{13}CO_2/^{12}CO_2$ steady-state labelling and gas exchange. *New Phytologist* **172**: 544–553.

Hahn V, Högberg P, Buchmann N (2006) ^{14}C — a tool for separation of autotrophic and heterotrophic soil respiration. *Global Change Biology* **12**: 972–982.

Hanson PJ, Edwards NT, Garten CT, Andrews JA (2000) Separating root and soil microbial contributions to soil respiration: a review of methods and observations. *Biogeochemistry* **48**: 115–146.

Harned HS, Davis R (1943) The ionization constant of carbonic acid in water and the solubility of carbon dioxide in water and aqueous salt solutions from 0 to 50°. *Journal of the American Chemical Society* **65**: 2030–2037.

Harned HS, Scholes SR (1941) The ionization constant of HCO_3^- from 0 to 50°. *Journal of the American Chemical Society* **63**: 1706–1709.

Hawkes CV, Hartley IP, Ineson P, Fitter AH (2008) Soil temperature affects carbon allocation within arbuscular mycorrhizal networks and carbon transport from plant to fungus. *Global Change Biology* **14**: 1181–1190.

Heinemeyer A, Ineson P, Ostle N, Fitter AH (2006) Respiration of the external mycelium in the arbuscular mycorrhizal symbiosis shows strong dependence on recent photosynthates and acclimation to temperature. *New Phytologist* **171**: 159–170.

Hendrey GR, Ellsworth DS, Lewin KF, Nagy J (1999) A free-air enrichment system for exposing tall forest vegetation to elevated atmospheric CO_2. *Global Change Biology* **5**: 293–309.

Högberg P, Read DJ (2006) Towards a more plant physiological perspective on soil ecology. *Trends in Ecology & Evolution* **21**: 548–554.

Högberg P, Högberg MN, Göttlicher SG, Betson NR, Keel SG, Metcalfe DB, Campbell C, Schindlbacher A, Hurry V, Lundmark T *et al.* (2008) High temporal resolution tracing of photosynthate carbon from the tree canopy to forest soil microorganisms. *New Phytologist* **177**: 220–228.

Jacquez J (1996) *Compartmental Analysis in Biology and Medicine.* Elsevier Publishing Company, Amsterdam, The Netherlands.

Johnson D, Leake JR, Ostle N, Ineson P, Read DJ (2002) In situ $^{13}CO_2$ pulse-labelling of upland grassland demonstrates a rapid pathway of carbon flux from arbuscular mycorrhizal mycelia to the soil. *New Phytologist* **153**: 327–334.

Kanemasu ET, Powers WL, Sij JW (1974) Field chamber measurements of CO_2 flux from soil surface. *Soil Science* **118**: 233–237.

Kayler ZE, Sulzman EW, Marshall JD, Mix A, Rugh WD, Bond BJ (2008) A laboratory comparison of two methods used to estimate the isotopic composition of soil $\delta^{13}CO_2$ efflux at steady state. *Rapid Communications in Mass Spectrometry* **22**: 2533–2538.

Keel SG, Siegwolf RTW, Körner C (2006) Canopy CO_2 enrichment permits tracing the fate of recently assimilated carbon in a mature deciduous forest. *New Phytologist* **172**: 319–329.

Keeling CD (1958) The concentration and isotopic abundances of atmospheric carbon dioxide in rural areas. *Geochimica et Cosmochimica Acta* **13**: 322–334.

Klapp E (1971) *Wiesen und Weiden.* Paul Parey, Berlin, Germany.

Klengel T, Liang WJ, Chaloupka J, Ruoff C, Schröppel K, Naglik JR, Eckert SE, Mogensen EG, Haynes K, Tuite MF *et al.* (2005) Fungal adenylyl cyclase integrates CO_2 sensing with cAMP signaling and virulence. *Current Biology* **15**: 2021–2026.

Kusian B, Sültemeyer D, Bowien B (2002) Carbonic anhydrase is essential for growth of *Ralstonia eutropha* at ambient CO_2 concentrations. *Journal of Bacteriology* **184**: 5018–5026.

Kuzyakov Y (2006) Sources of CO_2 efflux from soil and review of partitioning methods. *Soil Biology & Biochemistry* **38**: 425–448.

Lattanzi FA, Schnyder H, Thornton B (2004) Defoliation effects on carbon and nitrogen substrate import and tissue-bound efflux in leaf growth zones of grasses. *Plant Cell and Environment* **27**: 347–356.

Leadley PW, Drake BG (1993) Open top chambers for exposing plant canopies to elevated CO_2 concentration and for measuring net gas-exchange. *Vegetatio* **104**: 3–15.

Leake JR, Ostle NJ, Rangel-Castro JI, Johnson D (2006) Carbon fluxes from plants through soil organisms determined by field $^{13}CO_2$ pulse-labelling in an upland grassland. *Applied Soil Ecology* **33**: 152–175.

Lehmeier CA (2008) The turnover of respiratory carbon pools in grass plants - assessment by dynamic ^{13}C labeling and compartmental analysis of tracer kinetics in respired CO_2. Phd thesis, Technische Universität München, München, Germany.

Lehmeier CA, Schäufele R, Schnyder H (2005) Allocation of reserve-derived and currently assimilated carbon and nitrogen in seedlings of *Helianthus annuus* under subambient and elevated CO_2 growth conditions. *New Phytologist* **168**: 613–621.

Lehmeier CA, Lattanzi FA, Schäufele R, Wild M, Schnyder H (2008) Root and shoot respiration of perennial ryegrass are supplied by the same substrate pools: assessment by dynamic ^{13}C labelling and compartmental analysis of tracer kinetics. *Plant Physiology* **148**: 1148–1158.

Lehmeier CA, Lattanzi FA, Schäufele R, Schnyder H (2010) Nitrogen deficiency increases the residence time of respiratory carbon in the respiratory substrate supply system of perennial ryegrass. *Plant Cell and Environment* doi: 10.1111/j.1365-3040.2009.02058.x.

Lemaire G, Chapman D (1996) Tissue flows in grazed plant communities. *In* J Hodgson, AW Illius, eds, *The Ecology and Management of Grazing Systems.* Cab International, Wallington, UK, pp 3–36.

Lewin KF, Hendrey GR, Nagy J, LaMorte RL (1994) Design and application of a free-air carbon-dioxide enrichment facility. *Agricultural and Forest Meteorology* **70**: 15–29.

Liu L, Hoogenboom G, Ingram KT (2000) Controlled-environment sunlit plant growth chambers. *Critical Reviews in Plant Sciences* **19**: 347–375.

Livingston GP, Hutchinson GL (1995) Enclosure-based measurement of trace gas exchange: applications and sources of error. *In* PA Madson, RC Harriss, eds, *Biogenic Trace Gases: Measuring Emissions From Soil and Water.* Blackwell Science, Oxford, UK, pp 14–51.

Lötscher M, Klumpp K, Schnyder H (2004) Growth and maintenance respiration for individual plants in hierarchically structured canopies of *Medicago sativa* and *Helianthus annuus*: the contribution of current and old assimilates. *New Phytologist* **164**: 305–316.

Lund CP, Riley WJ, Pierce LL, Field CB (1999) The effects of chamber pressurization on soil-surface CO_2 flux and the implications for NEE measurements under elevated CO_2. *Global Change Biology* **5**: 269–281.

Matamala R, Gonzalez-Meler MA, Jastrow JD, Norby RJ, Schlesinger WH (2003) Impacts of fine root turnover on forest NPP and soil C sequestration potential. *Science* **302**: 1385–1387.

Meharg AA (1994) A critical review of labeling techniques used to quantify rhizosphere carbon-flow. *Plant and Soil* **166**: 55–62.

Midwood AJ, Thornton B, Millard P (2008) Measuring the ^{13}C content of soil-respired CO_2 using a novel open chamber system. *Rapid Communications in Mass Spectrometry* **22**: 2073–2081.

Miglietta F, Lanini M, Bindi M, Magliulo V (1997) Free air CO_2 enrichment of potato (*Solanum tuberosum* L.): design and performance of the CO_2-fumigation system. *Global Change Biology* **3**: 417–427.

Miglietta F, Peressotti A, Vaccari FP, Zaldei A, deAngelis P, Scarascia-Mugnozza G (2001) Free-air CO_2 enrichment (FACE) of a poplar plantation: the POPFACE fumigation system. *New Phytologist* **150**: 465–476.

Millington RJ (1959) Gas diffusion in porous media. *Science* **130**: 100–102.

Mitsuhashi S, Ohnishi J, Hayashi M, Ikeda M (2004) A gene homologous to β-type carbonic anhydrase is essential for the growth of *Corynebacterium glutamicum* under atmospheric conditions. *Applied Microbiology and Biotechnology* **63**: 592–601.

Mogensen EG, Janbon G, Chaloupka J, Steegborn C, Fu MS, Moyrand F, Klengel T, Pearson DS, Geeves MA, Buck J *et al.* (2006) *Cryptococcus neoformans* senses CO_2 through the carbonic anhydrase Can2 and the adenylyl cyclase Cac1. *Eukaryotic Cell* **5**: 103–111.

Mook WG, Bommerson JC, Staverman WH (1974) Carbon isotope fractionation between dissolved bicarbonate and gaseous carbon dioxide. *Earth and Planetary Science Letters* **22**: 169–176.

Mora G, Raich JW (2007) Carbon-isotopic composition of soil-respired carbon dioxide in static closed chambers at equilibrium. *Rapid Communications in Mass Spectrometry* **21**: 1866–1870.

Nickerson N, Risk D (2009a) Physical controls on the isotopic composition of soil-respired CO_2. *Journal of Geophysysical Research* **114:** doi:10.1029/2008JG000766.

Nickerson N, Risk D (2009b) Keeling plots are non-linear in non-steady state diffusive environments. *Geophysical Research Letters* **36:** doi:10.1029/2008GL036945.

Nickerson N, Risk D (2009c) A numerical evaluation of chamber methodologies used in measuring the $\delta^{13}C$ of soil respiration. *Rapid Communications in Mass Spectrometry* **23**: 2802–2810.

Nitschelm JJ, Lüscher A, Hartwig UA, Van Kessel C (1997) Using stable isotopes to determine soil carbon input differences under ambient and elevated atmospheric CO_2 conditions. *Global Change Biology* **3**: 411–416.

Nogués S, Tcherkez G, Cornic G, Ghashghaie J (2004) Respiratory carbon metabolism following illumination in intact french bean leaves using $^{13}C/^{12}C$ isotope labeling. *Plant Physiology* **136**: 3245–3254.

Ohlsson KEA, Bhupinderpal-Singh, Holm S, Nordgren A, Lövdahl L, Högberg P (2005) Uncertainties in static closed chamber measurements of the carbon isotopic ratio of soil-respired CO_2. *Soil Biology and Biochemistry* **37**: 2273–2276.

Ostle N, Ineson P, Benham D, Sleep D (2000) Carbon assimilation and turnover in grassland vegetation using an in situ $^{13}CO_2$ pulse labelling system. *Rapid Communications in Mass Spectrometry* **14**: 1345–1350.

Pataki DE, Ehleringer JR, Flanagan LB, Yakir D, Bowling DR, Still CJ, Buchmann N, Kaplan JO, Berry JA (2003) The application and interpretation of Keeling plots in terrestrial carbon cycle research. *Global Biogeochemical Cycles* **17:** doi:10.1029/2001GB001850.

Penman HL (1940) Gas and vapour movements in the soil I. The diffusion of vapours through porous solids. *Journal of Agricultural Science* **30**: 437–462.

Pepin S, Körner C (2002) Web-FACE: a new canopy free-air CO_2 enrichment system for tall trees in mature forests. *Oecologia* **133**: 1–9.

Pregitzer K, Loya W, Kubiske M, Zak D (2006) Soil respiration in northern forests exposed to elevated atmospheric carbon dioxide and ozone. *Oecologia* **148**: 503–516.

Ratcliffe RG, Shachar-Hill Y (2006) Measuring multiple fluxes through plant metabolic networks. *Plant Journal* **45**: 490–511.

Raven JA, Newman JR (1994) Requirement for carbonic-anhydrase activity in processes other than photosynthetic inorganic carbon assimilation. *Plant Cell and Environment* **17**: 123–130.

Reich PB, Tilman D, Craine J, Ellsworth D, Tjoelker MG, Knops J, Wedin D, Naeem S, Bahauddin D, Goth J *et al.* (2001) Do species and functional groups differ in acquisition and use of C, N and water under varying atmospheric CO_2 and N availability regimes? A field test with 16 grassland species. *New Phytologist* **150**: 435–448.

Rolston DE (1986) Gas diffusivity. *In* A Klute, ed, *Methods of Soil Analysis, Part 1: Physical and Mineralogical Methods.* Soil Science Society of America, pp 1089–1102.

Ryan MG, Law BE (2005) Interpreting, measuring, and modeling soil respiration. *Biogeochemistry* **73**: 3–27.

Ryle GJA, Cobby JM, Powell CE (1976) Synthetic and maintenance respiratory losses of $^{14}CO_2$ in uniculm barley and maize. *Annals of Botany* **40**: 571–586.

Ryser P, Urbas P (2000) Ecological significance of leaf life span among Central European grass species. *Oikos* **91**: 41–50.

Sanders GE, Clark AG, Colls JJ (1991) The influence of open-top chambers on the growth and development of field bean. *New Phytologist* **117**: 439–447.

Schnyder H (1992) Long-term steady-state labeling of wheat plants by use of natural $^{13}CO_2/^{12}CO_2$ mixtures in an open, rapidly turned-over system. *Planta* **187**: 128–135.

Schnyder H, Schäufele R, Lötscher M, Gebbing T (2003) Disentangling CO_2 fluxes: Direct measurements of mesocosm-scale natural abundance $^{13}CO_2/^{12}CO_2$ gas exchange, ^{13}C discrimination, and labelling of CO_2 exchange flux components in controlled environments. *Plant Cell and Environment* **26**: 1863–1874.

Schnyder H, Schäufele R, Wenzel R (2004) Mobile, outdoor continuous-flow isotope-ratio mass spectrometer system for automated high-frequency ^{13}C- and ^{18}O-CO_2 analysis for Keeling plot applications. *Rapid Communications in Mass Spectrometry* **18**: 3068–3074.

Schnyder H, Schwertl M, Auerswald K, Schäufele R (2006) Hair of grazing cattle provides an integrated measure of the effects of site conditions and inter-annual weather variability on $\delta^{13}C$ of temperate humid grassland. *Global Change Biology* **12**: 1–15.

Seibt U, Wingate L, Lloyd J, Berry JA (2006) Diurnally variable $\delta^{18}O$ signatures of soil CO_2 fluxes indicate carbonic anhydrase activity in a forest soil. *Journal of Geophysical Research-Biogeosciences* **111:** doi:10.1029/2006JG000177.

Søe ARB, Giesemann A, Anderson TH, Weigel HJ, Buchmann N (2004) Soil respiration under elevated CO_2 and its partitioning into recently assimilated and older carbon sources. *Plant and Soil* **262**: 85–94.

Staddon PL, Ostle N, Dawson LA, Fitter AH (2003) The speed of soil carbon throughput in an upland grassland is increased by liming. *Journal of Experimental Botany* **54**: 1461–1469.

Stitt M, Schulze ED (1994) Plant growth, storage, and resource allocation: from flux control in a metabolic chain to the whole-plant level, *In* ED Schulze, ed, *Flux Control in Biological Systems: From Enzymes to Populations and Ecosystems.* Academic Press, San Diego, CA, USA, pp 57–118.

Subke JA, Inglima I, Cotrufo MF (2006) Trends and methodological impacts in soil CO_2 efflux partitioning: a metaanalytical review. *Global Change Biology* **12**: 921–943.

Subke JA, Vallack HW, Magnusson T, Keel SG, Metcalfe DB, Högberg P, Ineson P (2009) Short-term dynamics of abiotic and biotic soil $^{13}CO_2$ effluxes after in situ $^{13}CO_2$ pulse labelling of a boreal pine forest. *New Phytologist* **183**: 349–357.

Taneva L, Pippen JS, Schlesinger WH, Gonzalez-Meler MA (2006) The turnover of carbon pools contributing to soil CO_2 and soil respiration in a temperate forest exposed to elevated CO_2 concentration. *Global Change Biology* **12**: 983–994.

Tcherkez G, Nogués S, Bleton J, Cornic G, Badeck F, Ghashghaie J (2003) Metabolic origin of carbon isotope composition of leaf dark-respired CO_2 in french bean. *Plant Physiology* **131**: 237–244.

Thode HG, Shima M, Rees CE, Krishnam KV (1965) ^{13}C isotope effects in systems containing carbon dioxide bicarbonate carbonate and metal ions. *Canadian Journal of Chemistry* **43**: 582–595.

Thornton B, Paterson E, Midwood AJ, Sim A, Pratt SM (2004) Contribution of current carbon assimilation in supplying root exudates of *Lolium perenne* measured using steady-state ^{13}C labelling. *Physiologia Plantarum* **120**: 434–441.

Torn MS, Davis S, Bird JA, Shaw MR, Conrad ME (2003) Automated analysis of $^{13}C/^{12}C$ ratios in CO_2 and dissolved inorganic carbon for ecological and environmental applications. *Rapid Communications in Mass Spectrometry* **17**: 2675–2682.

Trumbore S (2006) Carbon respired by terrestrial ecosystems — recent progress and challenges. *Global Change Biology* **12**: 141–153.

Van der Krift TAJ, Berendse F (2002) Root life spans of four grass species from habitats differing in nutrient availability. *Functional Ecology* **16**: 198–203.

Viktor A, Cramer MD (2005) The influence of root assimilated inorganic carbon on nitrogen acquisition/assimilation and carbon partitioning. *New Phytologist* **165**: 157–169.

Vogel JC, Grootes PM, Mook WG (1970) Isotopic fractionation between gaseous and dissolved carbon dioxide. *Zeitschrift für Physik* **230**: 225–238.

White RP, Murray S, Rohweder M (2000) *Pilot Analysis of Global Ecosystems: Grassland Ecosystems.* World Resources Institute, Washington, DC, USA.

Wingate L, Seibt U, Maseyk K, Ogee J, Almeida P, Yakir D, Pereira JS, Mencuccini M (2008) Evaporation and carbonic anhydrase activity recorded in oxygen isotope signatures of net CO_2 fluxes from a mediterranean soil. *Global Change Biology* **14**: 2178–2193.

Zanetti S, Hartwig UA, Lüscher A, Hebeisen T, Frehner M, Fischer BU, Hendrey GR, Blum H, Nösberger J (1996) Stimulation of symbiotic N_2 fixation in *Trifolium repens* L. under elevated atmospheric pCO_2 in a grassland ecosystem. *Plant Physiology* **112**: 575–583.

Zobitz JM, Keener JP, Schnyder H, Bowling DR (2006) Sensitivity analysis and quantification of uncertainty for isotopic mixing relationships in carbon cycle research. *Agricultural and Forest Meteorology* **136**: 56–75.

Candidate's individual contribution

Chapter 2

Gamnitzer U, Schäufele R, Schnyder H (2009) Observing ^{13}C labelling kinetics in CO_2 respired by a temperate grassland ecosystem
New Phytologist **184:** 376–386

The candidate developed independently the research question and story of this paper. She conducted the measurements of chamber characaterisation and tracer kinetics, analysed, interpreted and discussed the results. She composed the graphs and wrote the first draft and revised the paper. Overall, the candidate contributed about 90% to the completion of the entire article.

Chapter 3

Gamnitzer U. Non-steady-states of the soil CO_2 pool affect measurements of soil respiration: A quantitative investigation of the underlying mechanisms

The candidate defined the research question and developed the story of this chapter. She designed and conducted the measurements. Modelling of soil CO_2 diffusion was based on a discussion with D.R. Bowling and A.B. Moyes (both University of Utah, Salt Lake City, UT, USA). The candidate implemented and independently extended the model, and performed the model runs. She analysed, interpreted and discussed the results. She composed the graphs and wrote the paper. Submission of this chapter to a peer-reviewed journal for publication is purposed. It is intended to include D.R. Bowling and A.B. Moyes as co-authors after further discussion.